New York State Water Resources Institute
Annual Technical Report
FY 2017

Introduction

The Mission of the New York State Water Resources Institute (WRI) is to improve the management of water resources in New York State and the nation. As a federally and state mandated institution located at Cornell University, WRI is uniquely situated to access scientific and technical resources that are relevant to New York State's and the nation's water management needs. WRI collaborates with regional, state, and national partners to increase awareness of emerging water resources issues and to develop and assess new water management technologies and policies. WRI connects the water research and water management communities. Collaboration with New York partners is undertaken in order to: 1) Build and maintain a broad, active network of water resources researchers and managers, 2) Bring together water researchers and water resources managers to address critical water resource problems, and 3) Identify, adopt, develop and make available resources to improve information transfer on water resources management and technologies to educators, managers, policy makers, and the public.

Research Program Introduction

The NYS WRI's FY2017 competitive grants research program was conducted in partnership with the NYS Department of Environmental Conservation (DEC) Hudson River Estuary Program (HREP). The overall objective of this program is to bring innovative science to watershed planning, management and policy. In FY2017 research was sought that fit within the context of New York State's concerns about aging public water resources infrastructure and related economic constraints on public investment. Additionally, competitive funding was directed toward projects that incorporated analysis of climate change and/or extreme weather and their impacts on communities, ecosystems, and infrastructure. The specific areas of interest for the FY2016 grants program solicitation were: 1) The current state and effectiveness of water-resource infrastructure including water supply and wastewater treatment facilities; related distribution networks and source watersheds; natural and "green" infrastructure; riparian corridors; decentralized treatment installations; dams; culverts and bridges; constructed wetlands; etc.; at providing water services regionally at reasonable cost; and understanding the connections between watershed protection, drinking water management, and aquatic life needs; 2) Effects of climate change and extreme weather impacts on New York's communities; assessment of the resilience of ecosystems, infrastructure, communities, and governance institutions to climate change and/or development of strategies to increase such resiliency; 3) Integration of scientific, economic, planning, governmental and/or social expertise to build comprehensive strategies for local infrastructure and watershed managers; 4) Outreach methods that enhance the communication and impact of science-based innovation to water resource managers, policy makers, and the public; we are especially open to novel or innovative methods; and 5) The relationship between management in the Hudson River watershed and the estuary ecosystem's fish and wildlife, and water quality and quantity.

Projects were evaluated by a panel consisting of 3 WRI staff representatives, 1 Cornell University faculty member, 1 staff member from the NYS Department of Environmental Conservation, 1 Sea Grant staff member, and 2 representatives from other NY-based academic institutions. Five research projects were initiated with 104b base funding, while another four were initiated and funded through DEC sources that WRI leverages with its base federal grant. For FY2017, 104b-funded projects include:

1. Ileana Dumitriu, Hobart & William Smith Colleges: "Remote Sensing, Harmful Algal Blooms, Spectroscopy, Unmanned Aerial Systems"

2. Chester Zarnoch, CUNY-Baruch College: "Quantifying the ecosystem services of nitrogen removal and carbon sequestration in restored urban tidal wetlands"

3. Kiyoko Yokota, SUNY Oneonta: "Otsego Lake Water Quality Constant Monitoring System"

4. David Richardson, SUNY New Paltz: "Variability in water quality and the effect of climate change and teleconnections on lake thermal structure in the Sky Lakes of Shawangunk Ridge"

5. Scott Steinschneider, Cornell University: "Dynamic sediment-discharge rating curve models to support climate-smart management of water quality in the New York City water supply system"

Innovative water treatment by chitosan modified diatomaceous earth for small public water systems in rural areas

Basic Information

Title:	Innovative water treatment by chitosan modified diatomaceous earth for small public water systems in rural areas
Project Number:	2016NY228B
Start Date:	3/1/2016
End Date:	8/31/2017
Funding Source:	104B
Congressional District:	NY-22
Research Category:	Water Quality
Focus Categories:	Treatment, Water Supply, Toxic Substances
Descriptors:	None
Principal Investigators:	Xinchao Wei

Publications

1. Xinchao Wei, Nathaniel Cady, Aaron Mosier “Synergistic effect of metal combinations in ferrite nanoparticles for As (III&V) removal,” The 252th ACS National Meeting & Expo, Aug. 21-25, 2016, Philadelphia, PA
2. Xinchao Wei, Carolyn Rodak, Robyn Christoferson, Stephen Nguyen “Contaminants removal by chitosan modified diatomaceous earth for small public water systems”, Accepted by The 2017 AEESP Research and Education Conference, June 20-22, 2017, Ana Arbor, MI

NEW YORK STATE WATER RESOURCES INSTITUTE

Department of Biological and Environmental Engineering

230 Riley-Robb Hall, Cornell University
Ithaca, NY 14853-5701
http://wri.cals.cornell.edu

Tel: (607) 254-7163
Fax: (607) 255-4449
Email: nyswri@cornell.edu

Innovative water treatment by chitosan modified diatomaceous earth (DE) for small public water systems in rural areas

Xinchao Wei, Ph.D., P.E.
College of Engineering SUNY Polytechnic Institute
100 Seymour Road, Utica, NY 13502

Abstract

Small public water systems play a vital role in providing safe drinking water to many rural areas in many states in the U.S. In view of the growing amounts and types of pollutants, providing safe drinking water is becoming increasingly difficult for small public water systems because of their unique geographical, financial, technical and operational constraints. The objective of this study was to develop a drinking water treatment technology for resource-constrained small public water systems using chitosan modified diatomaceous earth (DE) to remove a group of dissolved contaminants (natural organic matters, arsenic, and nitrate). Chitosan is an effective biosorbent for various dissolved contaminants mainly due to its high density amino groups and hydroxyl groups. DE of different sizes and permeability was modified by a chitosan to achieve the uniform thin coating on DE surfaces. The new adsorbent had the unique properties of both DE (good mechanical strength, large surface area, and good permeability) and chitosan (ubiquitous biopolymer with outstanding versatile adsorption capacity). The adsorption performance in removing the target contaminants was examined by batch adsorption tests.

Three Summary Points of Interest

- Chitosan modified DE showed effective removal of natural organic matters, precursors of disinfection byproduct.
- Chitosan modified DE is more effective in removing arsenate than arsenite.
- The performances of all chitosan modified DE in removing nitrate were not significant.

Keywords: Chitosan, diatomaceous earth, small water systems, arsenic, natural organic matter

Introduction

Diatomaceous earth (DE), or diatomite, is commonly used in water filtration as filter media for small water systems identified by the EPA (EPA, 1997). There are nearly 200 DE water treatment plants in operation in the US (Bhardwaj and Mirliss, 2001). Actually, ~60% of DE produced in the U.S. is used for water filtration (USGS, 2007). DE filtration is effective in removing suspended solids as well as Giardia cysts, algae and asbestos (EPA, 1990). However, DE is not effective in removing dissolved contaminants (color, odor, taste, dissolved organics and inorganics) (WADOH, 2003; EPA, 1997). Chitosan is a cationic biopolymer derived from chitin, the second most abundant natural fiber (next to cellulose), which is found in the shells of shrimp and crab. Chitosan is an effective biosorbent for various dissolved contaminants mainly due to its high density amino groups (-NH2) and hydroxyl groups (-OH) (Bhatnagar and Sillanpää, 2009; Crini and Badot, 2008; Gerente et al., 2007; Varma et al., 2004; Guibal, 2004). Chitosan has the highest adsorption capacity among the biopolymers (Wan et al., 2010; Crini and Badot, 2008). Chitosan can be a low-cost adsorbent and has been used to remove dissolved organic contaminants (humic acid, fulvic acid, phenols, and dyes) and dissolved inorganics, such as metals (Cu, Cd, Hg, Ni, Zn, Pb, Cr, Al, As, and Mo etc.) and anions (sulfate, nitrate, fluoride), as summarized by Bhatnagar and Sillanpää (2009). The objectives of this proposed work are to develop a novel sustainable drinking water treatment technology suitable for small rural water systems by using chitosan modified DE

Methods

Chitosan with a low molecular weight was selected to modify the surface of DE so that a thin layer of chitosan with a high degree of uniformity was formed. Commercial DE from World Minerals® was used for the experiments. In consultation with the Oneida County Health Department (OCHD), the most common contaminants which can potentially cause maximum contaminant level (MCL) violations in the Mohawk Valley of New York state are arsenic and nitrate. OCHD also has great concern about disinfection byproducts (due to the presence of natural organic matters) because disinfection is the only treatment for many of its small rural water systems

The typical coating process will include: 1) pretreatment of DE (HCl, NaOH, or HF, if necessary); 2) dissolution of chitosan in acetic acid (2%) to prepare a dilute chitosan solution (1-4%); 3) surface modification of DE with chitosan by intensive mixing, sonication, or by elution of DE in a column with chitosan solution; 4) curing of chitosan on DE with NaOH; and 5) post-modification treatment, such as rinsing and drying. Batch studies will be conducted to examine the adsorption of target contaminants (natural organic matters, arsenic, nitrate and fluoride), alone and in combination, by agitating contaminated water (100 ml) dosed with predetermined amounts of the chitosan modified DE. After adsorption, modified DE will be separated from water by filtration and the contaminant levels in the filtrate will be analyzed to assess the adsorption performance.

Results & Discussion

Characterization of chitosan modified DE

The scanning electronic microscopy (SEM) image of chitosan modified DE is presented in Figure 1. The surface of DE was covered with a layer of chitosan. The surface coverage appeared to be uniform, although lumps of chitosan was found in certain locations.

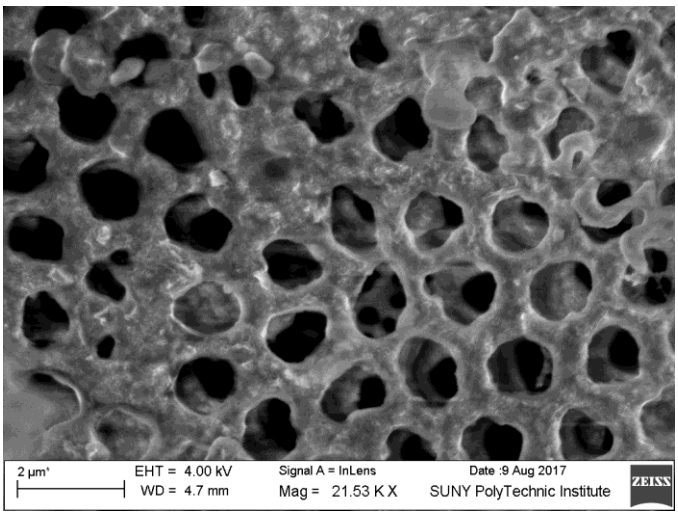

Figure 1. SEM image of typical chitosan modified DE

NOM Removal by chitosan modified DE

Humic acid (Sigma-Aldrich) was used as a surrogate for natural organic matters (NOM). UV-Vis

This report was prepared for the New York State Water Resources Institute (WRI) and was made possible through funding authorized under Section 104b of the Water Resources Research Act, administered by the US Geological Survey

spectrophotometer (Shimadzu UV-2600) was used to measure the concentrations of NOM using UV 254 as an indicate. DE modified with chitosan using various methods were able to remove NOM. The representative performance of chitosan modified DE in removing NOM is presented in Figure 2. It is evident that chitosan modified DE was effective in removing NOM. At a dose of 0.5 g/L, NOM concentration was reduced from 30 mg/L to less than 1 mg/L, representing >97% removal.

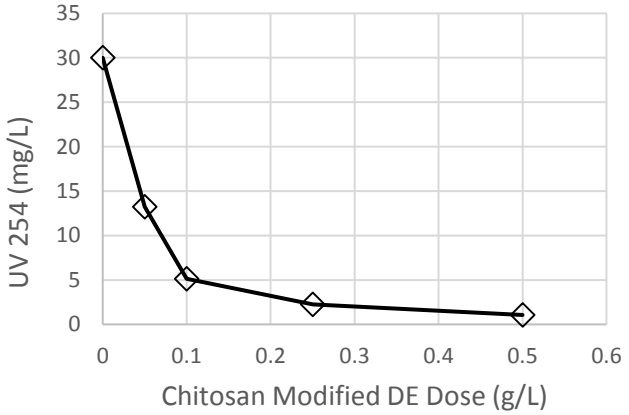

Figure 2. Removal of NOM using 2.5% chitosan coated DE at different doses. NOM initial concentration: 30 mg/L as humic acid.

Nitrate removal by chitosan modified DE

Great effort was made to evaluate the performance of nitrate removal using chitosan. Different coating methods and procedures were attempted. However, none of the products obtained could significantly remove nitrate. A typical nitrate removal performance is presented in Fig. 3. The nitrate concentration only decreased slightly at the highest dose (0.5 g/L). Therefore, it is concluded that chitosan modified DE was not effective in removing nitrate.

Arsenic removal by chitosan modified DE

Arsenic typically exists in water as arsenate (As(V)) and arsenite (As(III)). Both As species were studied in this projects. Presented in Figure 4 is the arsenate and arsenite removal using chitosan modified DE at different doses. The concentrations of both As species were reduced significantly. Because chitosan modified DE can remove both As species, the adsorption represents a unique advantage in removing As from water.

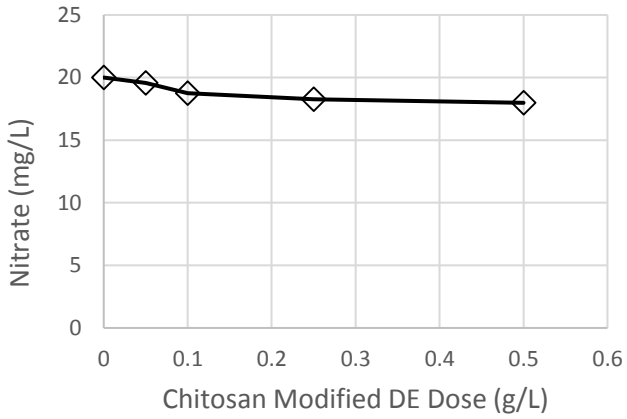

Figure 3. Removal of nitrate using 2.5% chitosan coated DE at different doses. Nitrate initial concentration: 20 mg/L.

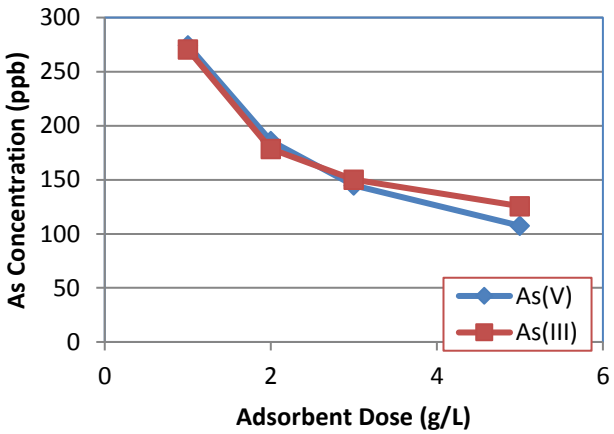

Figure 4. Arsenic Removal using chitosan modified DE at different doses. Chitosan content: 8%; Initial As concentration: 500 ppb.

The effect of pH on arsenite was presented in Figure 5. Clearly, pH had significant impacted on arsenite adsorption onto chitosan modified DE. Lower pH favored arsenite adsorption. Similar trend existed for arsenate. In addition, other competition anions in the water including chloride, nitrate, sulfate and carbonate had some interference with arsenic adsorption.

This report was prepared for the New York State Water Resources Institute (WRI) and was made possible through funding authorized under Section 104b of the Water Resources Research Act, administered by the US Geological Survey

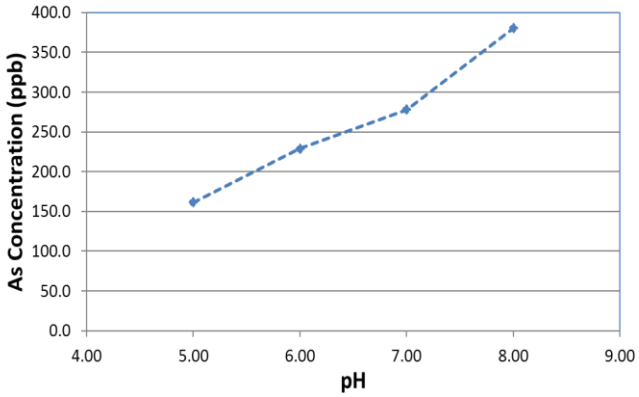

Figure 5. Effect of pH on arsenite adsorption onto chitosan modified DE.

Student Training

Three student was trained and partially funded by this project: Robyn Christoferson, Stephen Nguyen and Alex Eanniello. All students were trained in basic laboratory safety, surface modification, adsorption tests, water quality analysis, and data analysis.

Publications/Presentations

- Xinchao Wei, Carolyn Rodak, Robyn Christoferson, Stephen Nguyen "Contaminants removal by chitosan modified diatomaceous earth for small public water systems", The 2017 AEESP Research and Education Conference, June 20-22, 2017, Ana Arbor, MI
- Xinchao Wei, Nathaniel Cady, Aaron Mosier "Synergistic effect of metal combinations in ferrite nanoparticles for As (III&V) removal," The 252th ACS Wan, M.-W., Kan, C.-C., Rogel, B.D., Dalida, M.L.P., 2010. Adsorption of copper (II) and lead (II) ions from aqueous solution on chitosan-coated sand. Carbohyd. Polym. 80(3), 891–899.National Meeting & Expo, Aug. 21-25, 2016, Philadelphia, PA

References

1. Bhardwaj, V., Mirliss, M.J., 2001. Diatomaceous earth filtration for drinking water. Tech Brief. National Drinking Water Clearinghouse, Morgantown, WV.
2. Bhatnagar, A., Sillanpää, M., 2009. Applications of chitin- and chitosan-derivatives for the detoxification of water and wastewater — A short review. Adv. Colloid and Interf. Sci. 152, 26–38.
3. Crini, G., Badot, P.-M., 2008. Application of chitosan, a natural aminopolysaccharide, for dye removal from aqueous solutions by adsorption processes using batch studies: A review of recent literature. Prog. Polym. Sci. 33(4), 399-447.
4. EPA, 1990. Technologies for Upgrading or Designing New Drinking Water Treatment Facilities, EPA/625/4-89/023. EPA Office of Drinking Water, Cincinnati, OH.
5. EPA, 1997. Small System Compliance Technology List for the Surface Water Treatment Rule. EPA 815-R-97-002. EPA Office of Water, Washington, DC.
6. Gerente, C., Lee, V.K.C., Cloirec, P.Le., McKay, G., 2007. Application of Chitosan for the Removal of Metals From Wastewaters by Adsorption—Mechanisms and Models Review. Cri. Rev. Environ. Sci. Technol., 37(1), 41-127.
7. Guibal, E., 2004. Interactions of metal ions with chitosan-based sorbents: a review. Sep. Purif. Technol. 38, 43–74.
8. USGS, 2007. 2006 Minerals Yearbook Diatomite. United States Geological Survey, Washington, DC.
9. Varma, A.J., Deshpande, S.V., Kennedy, J.F., 2004. Metal complexation by chitosan and its derivatives: a Review. Carbohydr. Polym. 55(1),77-93.
10. WA DOH, 2003. Slow Sand Filtration and Diatomaceous Earth Filtration for Small Water Systems. DOH PUB. #331-204. Washington State Department of Health, Olympia, WA.
11. Wan, M.-W., Kan, C.-C., Rogel, B.D., Dalida, M.L.P., 2010. Adsorption of copper (II) and lead (II) ions from aqueous solution on chitosan-coated sand. Carbohyd. Polym. 80(3), 891–899.

This report was prepared for the New York State Water Resources Institute (WRI) and was made possible through funding authorized under Section 104b of the Water Resources Research Act, administered by the US Geological Survey

Conductivity and nutrient monitoring in surface water's of NY's Finger Lakes region

Basic Information

Title:	Conductivity and nutrient monitoring in surface water's of NY's Finger Lakes region
Project Number:	2016NY231B
Start Date:	3/1/2017
End Date:	2/28/2018
Funding Source:	104B
Congressional District:	NY-23
Research Category:	Water Quality
Focus Categories:	Water Quality, Surface Water, Solute Transport
Descriptors:	None
Principal Investigators:	Todd Walter

Publications

1. Morse, N., McPhillips, L., Shapleigh, J., Walter, M.T. (2017 In Review). The role of denitrification in stormwater detention basin treatment of nitrogen. Environmental Science and Technology
2. Lisboa, MS.; Schneider, R., Walter, MT. Landuse and drought effect on P loads at the Owasco Lake watershed, NY. AGU 2016
3. Georgakakos, C.B., Morris, C.K., Walter, M.T. (in press). Challenges and opportunities with on-farm research: total and soluble reactive stream phosphorus before and after implementation of a cattle-exclusion, riparian buffer. Frontiers in Environmental Science, section Soil Processes: Riparian Buffer Special Ed.

NEW YORK STATE WATER RESOURCES INSTITUTE

Department of Biological and Environmental Engineering

230 Riley-Robb Hall, Cornell University
Ithaca, NY 14853-5701
http://wri.cals.cornell.edu

Tel: (607) 254-7163
Fax: (607) 255-4449
Email: nyswri@cornell.edu

Watershed management plans and modeling in Cayuga and Owasco Lakes

DRAFT PROGRESS REPORT

Introduction

In the Finger Lakes region of upstate NY, there are a variety of surface waters with quality that ranges from nearly pristine to impaired, as well as watersheds that range from urban to agricultural. A regional effort is needed to both monitor and model these surface waters to better understand the driving factors behind nutrient impairment. The need for this is further highlighted and driven by the occurrence of harmful algal bloom outbreaks in the area (REF).

Cayuga and Owasco Lakes, two of the eleven Finger Lakes, are currently the subjects of a Total Maximum Daily Load (TMDL) and Nine Element Plan (9E Plan), respectively. Central to both the TMDL and 9E Plan processes in the identification and modeling of point and nonpoint source pollution loads to the waterbody. However, who is involved in the creation and interpretation of the model, and how the model is ultimately used, differs between the two methods (Table 1).

Table 1, adapted from
https://www.dec.ny.gov/chemical/103264.html

Attribute	9E Plan	TMDL
Clean Water Act guidance	Section 319(h)	Section 303(d)
Pollutant sources	Focus on nonpoint sources	Focus on point sources
Implementation plan	Required	Optional, but included in TMDLs prepared by NYS DEC
Public comment period	None - public participation throughout plan development	Required
Agency approval	NYS DEC	EPA
Funding eligibility	State and federal	State and federal

This report contains the modeling completed as part of the Cayuga Lake TMDL, and information regarding data collection in support of the Owasco Lake modeling component of the 9E Plan. Ultimately, these two efforts will be compared to determine whether there is a difference in the way the model is applied.

Results & Discussion

Cayuga Lake TMDL model

Overview

We developed a SWAT v2012 model for the Cayuga Lake watershed to 1) estimate current precipitation driven discharge, total suspended solids (TSS), Nitrate + Nitrite (NO_X) and total phosphorus (TP) loading to Cayuga Lake, and 2) to evaluate best management practices in reducing TP loading to Cayuga Lake.

Model development and calibration was first performed for the Fall Creek watershed, a large tributary to the south end of Cayuga Lake. Fall Creek benefits from an extensive period of record of observed precipitation (NRCC, 2016), streamflow (USGS, 2016), and estimated water quality constituents (Prestigiacomo, 2016). Further, details on the spatial and temporal distributions of agricultural fertilizer applications were available for the Fall Creek watershed. These schedules were determined after discussions with experts from a number of county Soil and Water Conservation Districts (SWCDs) in the Finger Lakes region (K. Czymmck et al., personal communication, May 2015). This high level of data availability allows for more precise estimates of hydrologic model parameters that must be determined through calibration. Hydrologic parameters defining the precipitation-runoff response of the watershed derived from calibration of the Fall Creek watershed were then extrapolated to the entire Cayuga Lake watershed.

Known fertilizer spreading schemes for the Fall Creek watershed were extrapolated to the entire Cayuga Lake watershed. We assumed that the temporal distribution of fertilizer applications throughout the Cayuga Lake watershed was consistent with the management practices within Fall Creek. Further we assumed that the total mass of fertilizer applied was proportional based on area by land use. We assumed that all row crops throughout the watershed were actively fertilized as in Fall Creek with the same mass per unit area. We similarly assumed that the same proportion of pastures throughout the watershed received fertilizer spreading schedules defined for Fall Creek.

Hydrologic Model Selection and Development

Bouraoui and Grizzetti (2014) review existing hydrologic models employed to estimate nutrient losses from agricultural land and the efficacy of nutrient runoff mitigation measures. They identify the Soil and Water Assessment Tool (SWAT) as the model is 1) generally more physically based than existing models, 2) spatially and temporally distributed, 3) capable of complex fertilizer application strategies, and 4) capable of complex crop management strategies. Panagopoulos et al. (2011) demonstrate that even under data-poor conditions, prediction of spatially distributed nutrient losses with SWAT still provides some value due to the physical-basis and theoretical underpinnings of the nutrient loss models. For these reasons we use the SWAT model to simulate N and P watershed losses and to evaluate the efficacy of nutrient loss control measures. We developed the SWAT model using SWAT v2012 through the ArcSWAT extension of ESRI ArcGIS.

Table 2 – Summary of data used for model parameterization

Data	Source
30 m National Elevation Dataset (NED) digital elevation model	USGS, 2016a
land-use	National Land Cover Database (NLCD), Fry et al, 2011
30-m 2009 New York Cropland Data Layer	USDA, 2010
Soils layer	TopoSWAT, (Fuka and Easton, 2016)
Fertilizer application schedule	Soil and Water Conservation Districts (K. Czymmck et al., personal communication, May 2015)

We utilize 30 m National Elevation Dataset (NED) digital elevation model to define watershed land surface elevations (USGS, 2016a). We obtain land-use information from the National Land Cover Database (NLCD) (Fry et al, 2011) and 30-m 2009 New York Cropland Data Layer (USDA, 2010). The NLCD dataset was modified to include more specific agricultural land uses common to the Finger Lakes region of NYS such as vineyards, orchards, and vegetable farms. These additional agricultural data were obtained from the 2009 New York Cropland Data Layer at a resolution of 30 meters (USDA et al., 2010). One land use data set was used for the entire modeling period (1998-2010). Population growth in the watershed is consistent with this small increase in roadways; between 1950 and 1980 population increased by 10% each decade and

This report was prepared for the New York State Water Resources Institute (WRI) and was made possible through funding authorized under Section 104b of the Water Resources Research Act, administered by the US Geological Survey

from 1980 to present there has been a 5% increase in population in each decade (Forstall, 1995). Based on these data we can assume that land use has not appreciably changed over the modeling period (1998-2010). SWAT Hydrologic Response Units (HRUs) were determined by a unique combination of landuse, soils (which includes a topographic index class), slope, and subbasin. Land use thresholds were not used to determine HRUs in the final model to preserve all types of agriculture included in the land use datasets.

A soils layer was built using TopoSWAT (Fuka and Easton, 2016). TopoSWAT is an automated ArcMap tool that calls upon the Digital Soil Map of the World and includes a soil wetness class to give a more accurate representation of soil type and its propensity to generate runoff as defined by VSA hydrology (Fischer et al., 2008). We utilize SWAT-VSA (Variable Source Area) (Easton et al. 2008) to redistribute the spatial pattern of runoff generation in NY, USA based on the TI concept. Redistribution of runoff generating characteristics was limited to a redistribution of the SWAT CN2 parameter.

Dairy manure is applied to all row crops and a subset of pastures within the Fall Creek watershed (Table 3). These schedules were determined after discussions with experts from a number of county Soil and Water Conservation Districts (SWCDs) in the Finger Lakes region (K. Czymmck et al., personal communication, May 2015). In these discussions we outlined four manure spreading schedules for pasture land and one for row crops. Dairy manure is defined as 0.7% NH_3 and 0.5% soluble P by mass (ASAE, 1998).

In order to incorporate fertilizer schedules (Table 3) into the SWAT framework, we assigned random HRUs, whose land use designation is Pasture, to 19 groups of three spatial sizes; 108 ha, 54 ha, and 400 ha. Twelve groups of 108 ha were assigned to Schedule 1; six groups of 54 ha were assigned to Schedule 2; and one group of 400 ha was assigned to Schedule 3 (Table 3). Each group under Schedules 1 and 2 were assigned a different month in which manure would be applied to them. As a result, each HRU received manure applications in only one month of the year. With this method we simulate the common practice of rotating the fields in which manure is spread. All HRUs designated as Row Crops were assigned to Schedule 4. We then applied manure to these groups as specified by the SWCD experts (Table 3).

Table 3. Current dairy manure application schedules within Fall Creek agricultural land

Land Use	Area (ha)	Dry Mass (kg/year)	NH_3 ($kg*ha^{-1}*yr^{-1}$)	TDP ($kg*ha^{-1}*yr^{-1}$)	Timing
Pasture	1300	4,290,000	23.1	16.5	year round (monthly)
Pasture	320	1,056,000	23.1	16.5	May - October
Pasture	400	3,680,000	64.4	46.0	May - October
Row Crops	5320	30,856,000	40.6	29.0	May - October

Fertilizer spreading schemes were extrapolated to the entire Cayuga Lake watershed. We assumed the same temporal distribution of fertilizer applications throughout the Cayuga Lake watershed was consistent with the management practices within Fall Creek. Further we assumed that the total mass of fertilizer applied was proportional based on land use. We assumed that all row crops throughout the watershed were actively fertilized as in Fall Creek. We assumed that the same proportion of pastures throughout the watershed received fertilizer spreading schedules defined for Fall Creek.

The entire Cayuga Lake model was developed following the same datasets and methodology as the Fall Creek watershed model. The Cayuga Lake watershed divisions were created to allow for a refined estimate of discharge and nutrient loading to the south end of Cayuga Lake based on the findings of DEC (2015). The model is capable of providing the total discharge and nutrient loading to Fall Creek from the major tributaries as well as the combined total discharge and nutrient loading from all contributing watersheds.

Model Corroboration

Table 4 – Summary of data used for model corroboration

Data	Source
observed daily flows in Fall Creek	USGS, 2016
estimated total suspended	Prestigiacomo et al.

This report was prepared for the New York State Water Resources Institute (WRI) and was made possible through funding authorized under Section 104b of the Water Resources Research Act, administered by the US Geological Survey

solids (TSS), NO_X (NO_3 + NO_2), Particulate Phosphorus (PP), and Total Dissolved Phosphorus (TDP) loads	(2016)
daily precipitation, and minimum and maximum air temperatures	Northeast Regional Climate Center weather station (NRCC, 2016)

We performed model corroboration for the period of 1998 – 2010. We corroborated our SWAT Fall Creek watershed model against observed daily flows (USGS, 2016) and estimated total suspended solids (TSS), NO_X (NO_3 + NO_2), Particulate Phosphorus (PP), and Total Dissolved Phosphorus (TDP) loads. Sediment and nutrient load collection methodology and flow-concentration relationships are presented in Prestigiacomo et al. (2016).

For model corroboration, we forced the Fall Creek model with daily precipitation, and minimum and maximum air temperatures measures at the Northeast Regional Climate Center weather station (NRCC, 2016). Relative humidity, solar radiation, and wind speed were solved internally by SWATs weather generator. These weather data are available from National Oceanic and Atmospheric Association (NOAA) Global Historical Climatology Network (GHCN) of weather stations. For this model we used the meteorological station (Number USC00304174) located at Cornell University in Ithaca, NY (NOAA, 2015) because of its location in the watershed and its long term data record.

We manually adjusted 19 SWAT model parameters for SWAT calibration (Table 2). Hydrologic parameters defining the precipitation-runoff response of the watershed derived from calibration of the Fall Creek watershed were then extrapolated to the entire Cayuga Lake watershed.

Table 5– SWAT parameters used in model corroboration

Parameter	Model	Calibrated Value	Units
SFTMP	Snowpack	1	˚C
SMTMP	Snowpack	0.5	˚C
SMFMX	Snowpack	2	mm H_2O /˚C * day
SMFMN	Snowpack	2	mm H_2O /˚C * day
TIMP	Snowpack	0.553	coefficient
ESCO	Water Balance	0.9	coefficient
EPCO	Water Balance	1	coefficient
SURLAG	Water Balance	0.2	days
CN_FROZ	Water Balance	0.000009	coefficient
GW_DELAY	Water Balance	1	days
ALPHA_BF	Water Balance	0.048	days
CN2	Water Balance	0.9*baseline	coefficient
USLE_K1	Sediment	0.275	coefficient
NPERCO	Nitrogen	0.4	coefficient
SDNCO	Nitrogen	1	coefficient
CDN	Nitrogen	1.4	coefficient
ERORGP	Phosphorus	0.285	coefficient
PHOSKD	Phosphorus	800	coefficient
PSP	Phosphorus	0.4	coefficient

Flow Corroboration

We corroborated the snowpack accumulation and melt through the adjustment of 5 parameters (Table 2). We corroborated the unsaturated zone dynamics, groundwater flow, and surface runoff through adjustment of 6 single value parameters and 1 distributed parameter (CN2) presented in Table 2. We manually adjusted parameter values until we were adequately reproducing both the seasonal loads of streamflow and obtaining acceptable Nash-Sutcliffe Model Efficiency (NSE) values as defined by Moriasi et al (2007).

TSS Corroboration

SWAT incorporates the Modified Universal Soil Loss Equation (MUSLE) which estimates daily suspended sediment load based on soil types, landscape practices, and daily rainfall. We corroborate the SWAT model for against estimates of daily TSS. The form of the MUSLE equation allows one to reduce calibration to a one parameter model. In this case we modify the soil erodibility factor (USLE_K) (Table 2).

NO_X Corroboration

We corroborate our model estimates of NO_X loads with daily estimates of in-stream NO_X loads. We adjust the following parameters for nitrogen loading: NPERCO, SDNCO, and CDN. We adopt the default values for nutrient parameters CMN, and RSDCO, which control the degradation of organic material, effecting both nitrogen and phosphorus nutrient cycling. We therefore primarily adjust the parameters related to

This report was prepared for the New York State Water Resources Institute (WRI) and was made possible through funding authorized under Section 104b of the Water Resources Research Act, administered by the US Geological Survey

denitrification and N percolation to calibrate the SWAT model to in-stream NO_X estimates.

Particulate and Total Dissolved Phosphorus Corroboration

SWAT estimates particulate phosphorus based on organic soil P concentrations and the estimated TSS reach loading. SWAT assumes that some proportion of the soil Organic P is attached to sediment and runs off. We adjusted the calibration parameter ERORGP which allows the user to define the concentration of organic P that is sediment bound.

SWAT estimates TDP surface runoff as a function of the surface 10 mm TDP concentration and the rate of surface runoff generation. We adjust the PHOSKD, soil phosphorus partitioning coefficient to match estimated TDP loads for Fall Creek.

Model Corroboration Results

Flow Corroboration

We obtain a daily NSE value above the recommended value of 0.5 (Moriasi et al 2007) for 10 of the 13 years used for model corroboration (Figure 3a). We note here that the commonly accepted NSE of 0.5 is defined for a monthly time step which is considerably more relaxed metric than NSE calculated at a daily time step.

Seasonally, we note that our observed reproduction of flow is good for all months with some overestimation occurring from spring snowmelt. We attribute this overestimate to the simplified approach to rain on frozen soils and soil thawing approximation within SWAT. SWAT assumes that soils remain frozen only for the duration that air temperatures are below 0˚C. When air temperatures exceed 0˚C soils begin infiltrating. In reality the snowmelt period likely occurs on soils that have not yet thawed resulting in a brief period of high runoff. In order to approximate this high runoff period of melt we decrease the CNFROZ parameter to generate more runoff during the spring melt period. The result is a slight over-prediction of the volume of spring snowmelt runoff (Figure 3b), and an under-estimate of the peak daily flow rate. This flow discrepancy affects the April loading of sediment and nutrients, and likely has a strong effect on the calculated NSE values.

Total Suspended Solids Corroboration

We manually adjust the USLE_K parameter until we sufficiently reproduce the cumulative TSS load estimate for the estimated load time period (Figure 3c). Daily estimates of TSS are highly variable due to uncertainty in the estimation of daily flow and the relative simplicity of the MUSLE equation. We observe that we are reproducing the seasonality of TSS loading with slight over-estimation of summer loads (Figure 3d). There is an underestimation of April TSS loads associated with spring snowmelt. As discussed in Section X, we are overestimating the volume of spring snowmelt, but slightly underestimating the peak daily flow rates.

NO_X Corroboration

Similar to the TSS, we observe that our model adequately estimates the long term trend in annual NO_X loading (Figure 3e), and reproduces the seasonality, but underestimates the spring snowmelt NO_X runoff (Figure 3f). SWAT assumes denitrification does not occur below some threshold soil moisture content. We corroborated NO_X stream loading through a reduction of the soil moisture threshold for the onset of denitrification. We assume that denitrification occurs when soils are at field capacity (SDNCO = 1.0). Other widely accepted theoretical models have demonstrated denitrification occurs at soil saturation levels less than field capacity (e.g. Parton et al. 1996). This simplified representation of denitrification likely produces an underestimate of the total NO_X lost to denitrification in drier soils.

Total Dissolved and Particulate Phosphorus

We manually adjust the PHOSKD and ERORGP parameters to reproduce the estimated TDP and PP loads for Fall Creek. We observe that the seasonality is well produced with a slight underestimation of spring P loads owing largely to the simplified snowmelt hydrology incorporated within SWAT (Figure 3 g-j).

This report was prepared for the New York State Water Resources Institute (WRI) and was made possible through funding authorized under Section 104b of the Water Resources Research Act, administered by the US Geological Survey

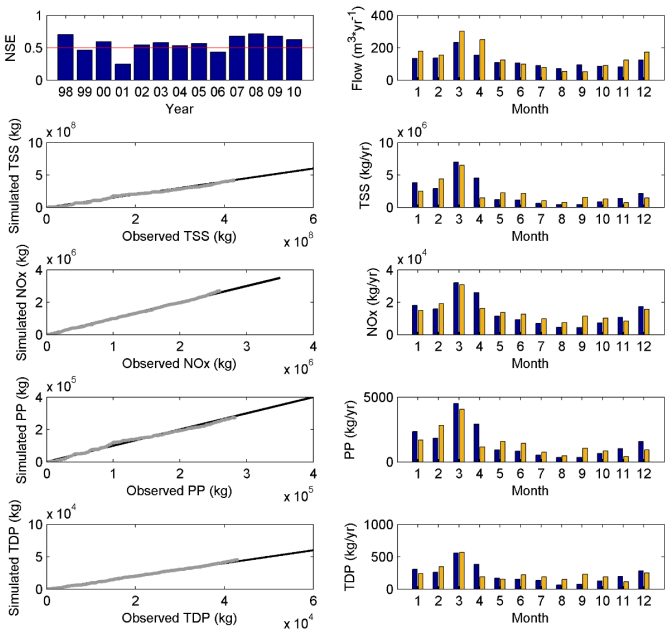

Figure 1 – Model corroboration for a) flow, c) total suspended solids, e) NOX, g) particulate phosphorus, and i) total dissolved phosphorus. Simulated (yellow), observed (blue).

Owasco Lake data collection

Table 6 – Summary of data used for model parameterization

Data	Source
30 m National Elevation Dataset (NED) digital elevation model	USGS, 2016a
land-use	National Land Cover Database (NLCD), Fry et al, 2011
30-m 2009 New York Cropland Data Layer	USDA, 2010
Soils layer	TopoSWAT, (Fuka and Easton, 2016)
Fertilizer application schedule	Soil and Water Conservation Districts (K. Czymmck et al., personal communication, May 2015)

Table 7 – Summary of data used for model corroboration

Data	Source
observed daily flows in Fall Creek	USGS, 2016
total suspended solids (TSS), NO_X (NO_3 + NO_2), Particulate Phosphorus (PP), and Total Dissolved Phosphorus (TDP) loads	Lisboa (unpublished)
daily precipitation, and minimum and maximum air temperatures	Northeast Regional Climate Center weather station (NRCC, 2016)

Policy Implications

TMDLs are required by Clean Water Act Section 303(d) in all cases where a waterbody is classified as "impaired" based on the water quality standards developed within a given state. TMDLs are approved at a national level by the EPA (REFS).

9E Plans are unique to New York State, but are based on national guidance. They formalize the nine minimum elements from the EPA's Clean Water Act section 319 Nonpoint Source Program's funding guidelines into a watershed management plan, and rely on the guidelines in *Handbook for Developing Watershed Plans to Restore and Protect our Waters* (EPA, 2008). Clean Water Section 319(h) funds go to states and tribal agencies to implement approved nonpoint source management plans. The funds are distributed annually according to a state-by-state allocation formula. The funding decisions are made by the states, which submit proposed funding plans to the EPA. Nonpoint source management plans must be consistent with grant eligibility requirements for the EPA to award funds to the state.

This report details the model development for the Cayuga Lake TMDL, and the data collection for later modelling use in the Owasco Lake 9E Plan. Future work will investigate how the interpretation of these two models differed, as driven by the watershed planning mechanism in which they were developed.

Outreach Comments

This report was prepared for the New York State Water Resources Institute (WRI) and was made possible through funding authorized under Section 104b of the Water Resources Research Act, administered by the US Geological Survey

Title

One graduate student presented at the Owasco Lake Association Meeting, March 1, 2017, Auburn, NY. Presentation title: *Landuses and Phosphorus Load into the Owasco Lake: Preliminary results from 2016 monitoring.*

Student Training

Five graduate students participated in the Cayuga and Owasco Lakes data collection and modeling.

Publications/Presentations

Publications

Georgakakos, C.B., Morris, C.K., Walter, M.T. (in press). *Challenges and opportunities with on-farm research: total and soluble reactive stream phosphorus before and after implementation of a cattle-exclusion, riparian buffer*. **Frontiers in Environmental Science, section Soil Processes: Riparian Buffer Special Ed.**

Presentations

Sustainable Dairy Systems: Food, Energy, Water. Georgakakos C. February 22, 2018. *Managing Best Management Practices*. (oral presentation)

Sustainable Dairy Systems: Food, Energy, Water. Lisboa M.S. February 22, 2018, Ithaca, NY. *Agricultural impact on phosphorus input to the Owasco Lake.* (oral presentation)

Finger Lakes Research Conference. Georgakakos C. November 17, 2017. *Evaluating effectiveness of best management practices at reducing phosphorus runoff from pastures* (poster presentation).

Finger Lakes Research Conference. Rosero-Lopez D., M. Sol Lisboa, M. Parker, M.T Walter. November 17, 2017. *Phosphorus concentrations and invertebrate communities in Owasco Lake tributaries* (poster presentation)

Finger Lakes Research Conference. Lisboa M.S. November 17, Geneva, NY. *Drought and Land-use effect on Phosphorus input to the Owasco Lake* (poster presentation)

Additional final reports related to water resource research are available at http://wri.cals.cornell.edu/news/research-reports

References

This report was prepared for the New York State Water Resources Institute (WRI) and was made possible through funding authorized under Section 104b of the Water Resources Research Act, administered by the US Geological Survey

Remote Sensing of Harmful Algal Blooms by Unmanned Aerial Systems (Drones)

Basic Information

Title:	Remote Sensing of Harmful Algal Blooms by Unmanned Aerial Systems (Drones)
Project Number:	2017NY237B
Start Date:	3/1/2017
End Date:	2/28/2018
Funding Source:	104B
Congressional District:	NY-23
Research Category:	Water Quality
Focus Categories:	Water Quality, Education, Toxic Substances
Descriptors:	None
Principal Investigators:	Ileana Dumitriu, John Halfman

Publications

There are no publications.

1. Title**: Remote Sensing of Harmful Algal Blooms by Unmanned Aerial Systems (Drones)**

2. Project type: **Education**

3. Focus categories: **Water Quality**

4. Research category: **Water Quality, Education, Toxic Substances**

5. Keywords: **Remote Sensing, Harmful Algal Blooms, Spectroscopy, Unmanned Aerial Systems**

6. Duration: **March 1, 2017 to February 28, 2018**

7. Funds requested: **$5,000**

8. Matching funds: **Not Applicable**

9. Principal investigators: **Ileana Dumitriu, John Halfman and Peter Spacher, Hobart and William Smith Colleges**

10. Congressional district: **23**

11. Abstract: Harmful Algal Blooms (HABs) from various blue-green algae species have added toxins to and thus degraded water quality in a growing list of New York's waterways. Concern is heightened in those waterways that supply drinking water and recreational services to the surround communities. The transient nature of HABs in both space and time result in monitoring challenges, and therefore adds to the difficulty in scientifically understanding the ecological criteria that trigger HABs. We propose to improve on our initial successes at monitoring algal blooms using drones by outfitting them with spectrometers and ultimately developing a reliable and low cost means to remotely detect and map HABs. The Finger Lakes Institute's water quality monitoring of the eight easternmost Finger Lakes of central and western New York provide a critical cost-savings partnership and an ideal natural laboratory to develop this new technology.

THIS PROJECT HAS RECEIVED A NO-COST-EXTENSION DUE TO DELAYS IN PROJECT FUNDING, AND DOES NOT CURRENTLY HAVE A PROGRESS REPORT

Variability in water quality and the effect of climate change and teleconnections on lake thermal structure in the Sky Lakes of Shawangunk Ridge

Basic Information

Title:	Variability in water quality and the effect of climate change and teleconnections on lake thermal structure in the Sky Lakes of Shawangunk Ridge
Project Number:	2017NY238B
Start Date:	3/1/2017
End Date:	2/28/2018
Funding Source:	104B
Congressional District:	NY-19
Research Category:	Water Quality
Focus Categories:	Ecology, Surface Water, Water Quality
Descriptors:	None
Principal Investigators:	David Richardson

Publications

There are no publications.

Progress Report
Dr. David Richardson
WRI small grant: 2017
Title: Variability in water quality and the effect of climate change and teleconnections on lake thermal structure in the Sky Lakes of Shawangunk Ridge

Research question: How have climatic drivers (i.e., climate change and teleconnections) affected lake temperatures and thermal stratification in the Sky Lakes?

We have worked with the Mohonk Preserve to quality analyze and check historic Mohonk Lake limnology data dating from 1983 to 2016. We have calculated annual and stratified season (hereafter summer) surface and deepwater temperature. Summer surface (epilimnion) is warming at ~0.5°C per decade (Fig. 1) – similarly, epilimion temperature during peak temperature is rising. The residuals appear to have a periodicity (Fig. 1, inset) that may relate to teleconnections (subdecadal scale climate oscillations like El Nino or North Atlantic Oscillation). Conversely, hypolimnion temperature is cooling at ~0.3°C per decade (Fig. 2). Interestingly, there were two extreme outliers on the figure, the first (1984) and last (2016) years of the dataset that otherwise followed the linear trend tightly. We will be examining these two years more closely to ensure they are real values. We also calculated the Schmidt stability of stratification which is the measure of work required to overcome density stratification and completely mix a lake (Klug et al. 2012) and is an indicator of how stable stratification is in a lake. This was calculated using Mohonk Lake bathymetry for each day with a temperature profiles. The annual maximum stratification is increasing over time at a rate of 2.3 J m^{-2} day^{-1} (Fig. 3). We also integrated the area under the stability curve for each year, giving a total for how stable the stratification was in days J m^{-2}. The overall increasing rapidly by ~40% from 1984 to 2016 (Fig. 4). Surprisingly, the phenology of stratification (initialization of stratification each spring, day of turnover each fall, day of peak stratification each summer) did not change significantly over the last 33 years. Similarly, the length of stratification (mean=206 days) did not change over time.

Research question: What drives variability in trophic state across the Sky Lakes?
We found three different levels of trophic status across the Sky Lakes that are close in proximity (<20km) across them all. Awosting is oligotrophic with low chlorophyll *a* (<2.5 µg/L), oxic hypolimnion (Fig. 5), low total phosphorus and total nitrogen concentrations (<4 µg/L and 50 µg/L) and high water clarity. Mohonk is mesotrophic with higher chlorophyll *a* (2.5-5 µg/L), anoxic hypolimnion (Fig. 5), moderate total phosphorus and total nitrogen concentrations (13 µg/L and 70 µg/L) and high water clarity. Minnewaska is oligotrophic/mesotrophic with low to moderate chlorophyll *a* (3 µg/L), hypoxic hypolimnion (Fig. 5), low total phosphorus and total nitrogen concentrations (4 µg/L and 40 µg/L) and high water clarity. The three lakes differ in their pH (Awosting is acidic, Minnewaska and Mohonk are close to neutral) and their food webs (Awosting has no fish, Minnewaska only has had fish introduced recently, and Mohonk has had fish stocked in the lake since the 1880s).

Research question: What is the extent of cyanobacterial presence across the Sky Lakes?
On two separate dates in June 2017, we sampled all three Sky Lakes on the northern Shawangunk Ridge for phytoplankton communities. Using settling columns, we identified 200 individuals in each sample and pooled the results for the two different dates. Chlorophyta (green algae) were the most common in all three lakes, followed by Bacillariophyta (diatoms) (Fig. 6). Cyanobacteria were present in only in Mohonk Lake (11% of total) – predominantly Anabaena spp (Fig. 6).

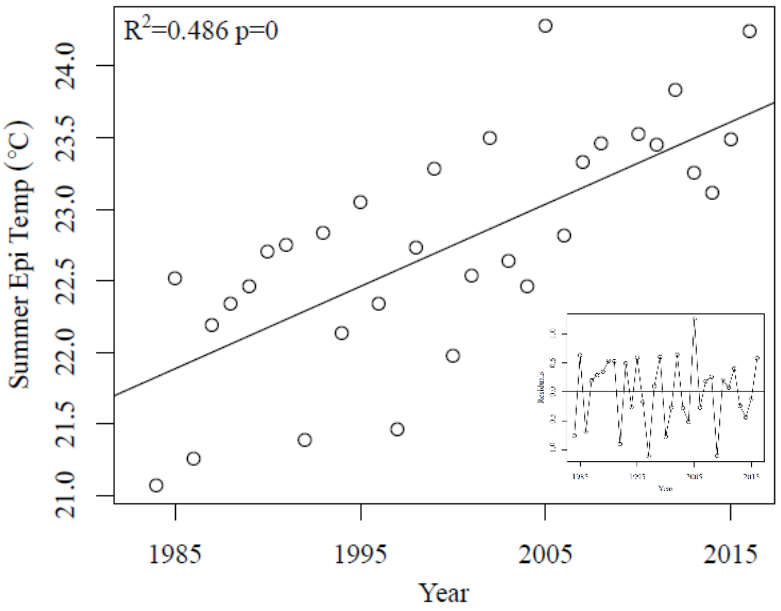

Figure 1. Summer annual average of epilimnion (1m – 3m) temperature in Mohonk over the last 33 years including significant linear regression (R^2 and p-value on graph). Residuals from the trend line are shown in the inset.

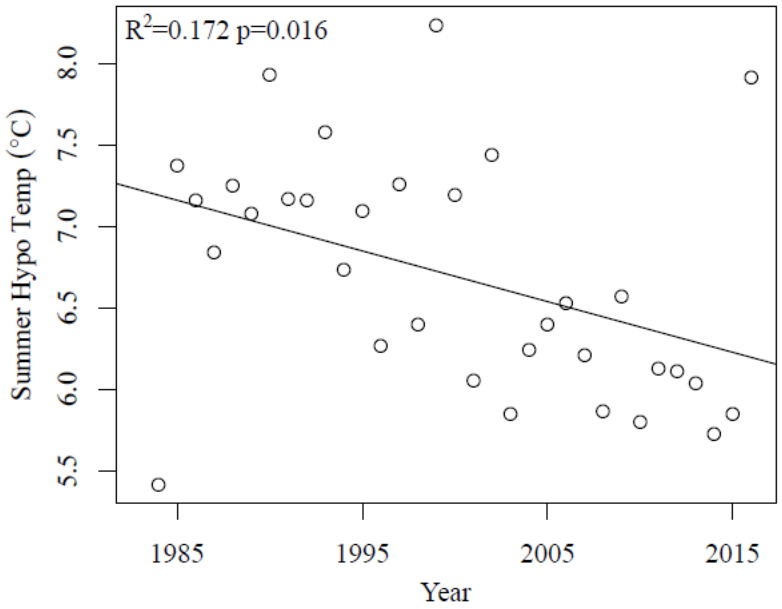

Figure 2. Summer annual average of hypolimnion (10m – 12m) temperature in Mohonk over the last 33 years including significant linear regression (R^2 and p-value on graph).

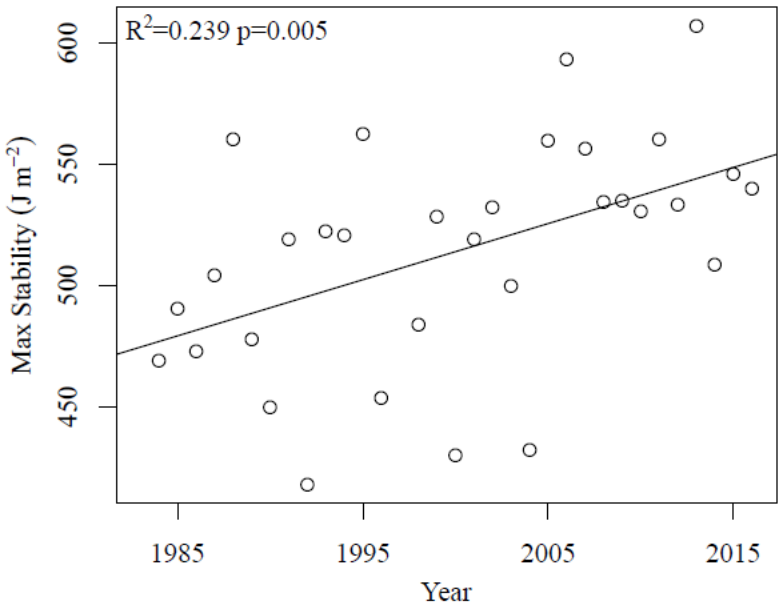

Figure 3. Maximum annual Mohonk Lake Schmidt stability of stratification over the last 33 years including significant linear regression (R^2 and p-value on graph).

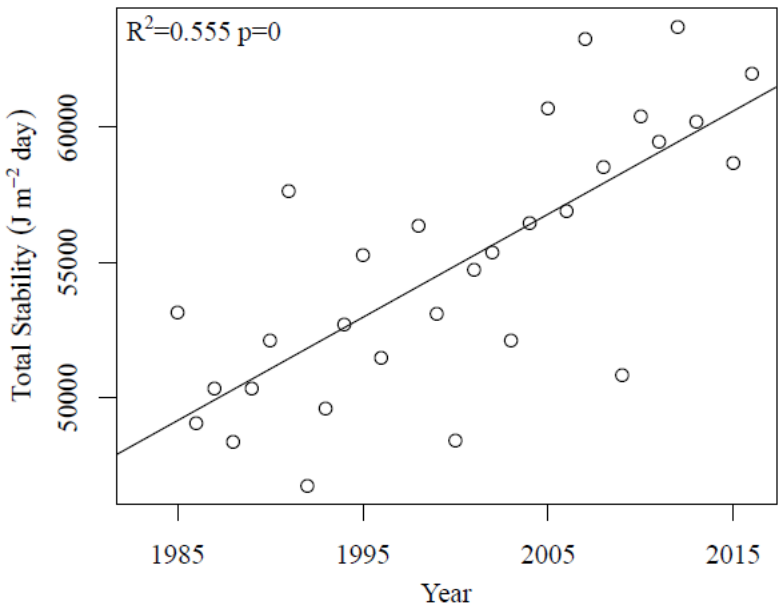

Figure 4. Total Mohonk Lake Schmidt stability integrated throughout the stratified period annually over the last 33 years including significant linear regression (R^2 and p-value on graph).

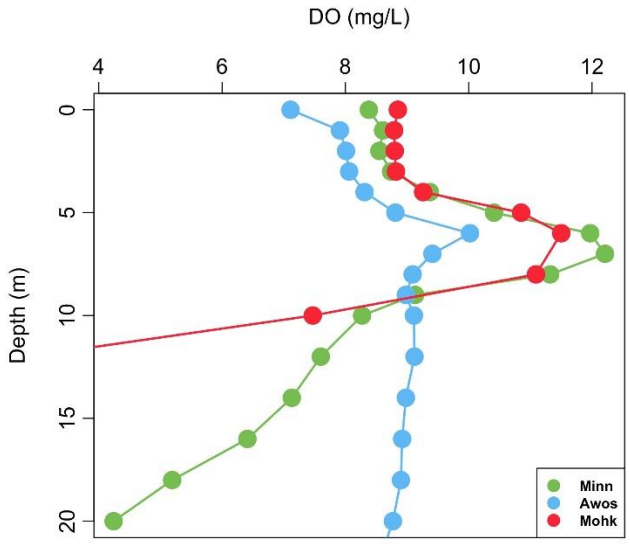

Figure 5. Dissolved oxygen profile taken on 19Jul2017 and 20Jul2017 for Minnewaska, Awosting, and Mohonk. Mohonk has the lowest DO concentration and Awosting has the greatest DO concentration at its deepest point.

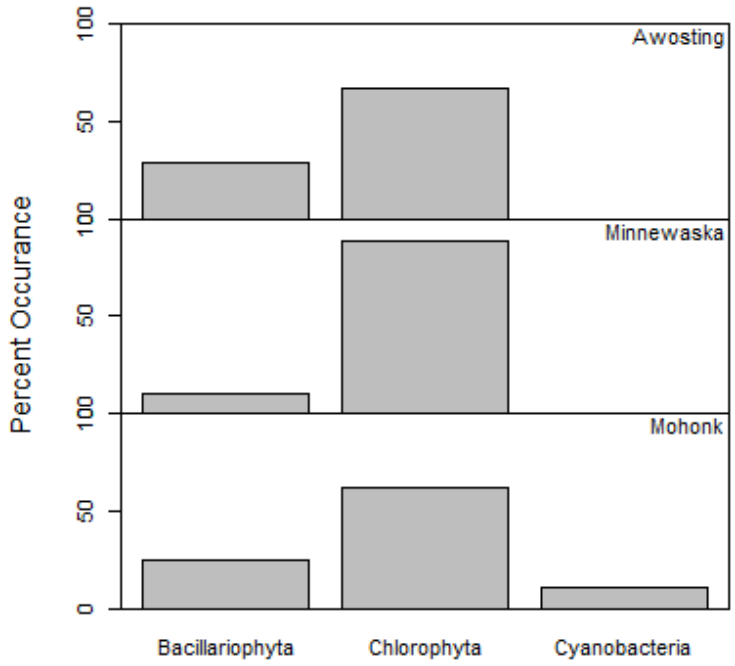

Figure 6. Community composition in three Sky Lakes on the northern Shawangunk Ridge. Three of the more common phyla are shown (bars will not add up to 100%).

Dynamic sediment-discharge rating curve models to support climate-smart management of water quality in the New York City water supply system

Basic Information

Title:	Dynamic sediment-discharge rating curve models to support climate-smart management of water quality in the New York City water supply system
Project Number:	2017NY239B
Start Date:	3/1/2017
End Date:	2/28/2018
Funding Source:	104B
Congressional District:	NY-23
Research Category:	Climate and Hydrologic Processes
Focus Categories:	Sediments, Floods, Water Supply
Descriptors:	None
Principal Investigators:	Scott Steinschneider

Publications

1. Ahn, K.-H., B. Yellen, and S. Steinschneider (2017), Dynamic linear models to explore time- varying suspended sediment-discharge rating curves, Water Resour. Res., 53, 4802–4820, doi:10.1002/2017WR020381.
2. Ahn, K-H, Steinschneider, S. (2017), Time-varying suspended sediment-discharge rating curves to estimate climate impacts on fluvial sediment transport. Hydrological Processes, 32, 102-117.

Final Technical Report for the New York Water Resources Institute

Dynamic sediment-discharge rating curve models to support climate-smart management of water quality in the New York City water supply system

Scott Steinschneider
Department of Biological and Environmental Engineering
Cornell University

Abstract

The research conducted in this work developed dynamic (i.e., time-varying) sediment–discharge rating curves for the Esopus Creek, a tributary in the Hudson River Estuary Basin and a major source of water supply for New York City (NYC). These dynamic rating curves were created to help the NYC Department of Environmental Protection (DEP) understand 1) how sediment yield per unit of streamflow has changed over time at multiple temporal scales (daily-decadal), 2) what aspects of climate variability are responsible for these fluctuations, and 3) how these fluctuations could be modeled under future climate scenarios. The analysis emphasized the lasting impact of major floods on the flow-sediment relationship. This information is critically important because high suspended sediment following major floods threatens the ability of DEP to meet the requirements of NYC's Filtration Avoidance Determination, which saves the city billions of dollars in avoided infrastructure costs for drinking water filtration. These events also disturb creek-side communities and aquatic ecosystems downstream on the Esopus Creek in Ulster County. This work will better enable NYC DEP to accurately generate and plan for scenarios of sedimentation under future climate with intensifying extreme events.

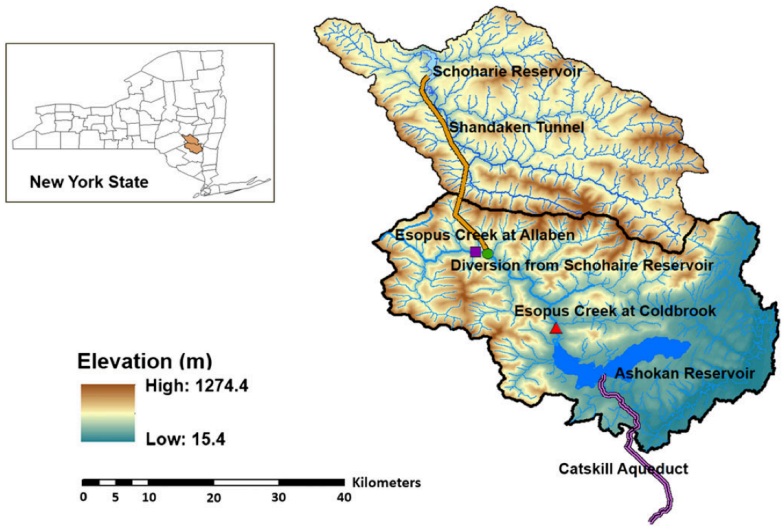

Figure 1. Map of project area.

Three Summary Points of Interest

- An application of the Dynamic Linear Model (DLM) framework in the Esopus Creek Watershed in NY revealed interesting flood-induced positive hysteresis in sediment yield.
- This behavior can be modeled using a latent variable regression model to support long-term climate change impact assessments.
- Long-term projections of sediment yield can vary substantially under future climate uncertainty depending on whether flood-induced positive hysteresis is considered.

Overview of Deliverables

Publications

Ahn, K.-H., B. Yellen, and S. Steinschneider (2017), Dynamic linear models to explore time-varying suspended sediment-discharge rating curves, Water Resour. Res., 53, 4802–4820, doi:10.1002/2017WR020381.

Ahn, K-H, Steinschneider, S. (2017), Time-varying suspended sediment-discharge rating curves to estimate climate impacts on fluvial sediment transport. Hydrological Processes, 32, 102-117.

Presentations

Steinschneider, S., and Ahn, K.-K. (2017), Dynamic linear models to explore time-varying sediment-discharge rating curves, *ASABE Annual International Meeting,* Presentation.

Ahn, K.-K., Yellen, B., and Steinschneider, S. (2017), Dynamic Rating Curves for Estimating Time-Varying Sediment Loads, *ASCE World Environmental and Water Resources Congress 2017*, Presentation.

Additional funding awarded related to this award

Time-Varying Sediment Yield Models to Support Long-Term Fluvial Sediment Estimates and Climate-Smart Planning in the Hudson River Watershed. Hudson River Foundation. Investigators: Scott Steinschneider, $49,000, May 1, 2017 – Apr 30. 2018

Training of Personnel

- 1 postdoctoral research supported (Kuk-Hyun Ahn)
- 1 semester-long undergraduate research project (Mackenzie Scheerer)

Background and Motivation

Sediment loadings in fluvial systems during and following extreme events place an enormous stress on critical water infrastructure throughout New York State (NYS). The challenge of excess suspended sediment following extremes is particularly relevant to the water supply system of New York City (NYC), where high suspended sediment and turbidity following major storms can exceed EPA maximum contaminant levels (MCLs) and threatens compliance with NYC's Filtration Avoidance Determination. These periods of elevated suspended sediment require the NYC Department of Environmental Protection (DEP) to actively and aggressively manage turbidity levels in their Catskill reservoir system, particular in the Ashokan Reservoir located on the Esopus Creek (see Fig. 1). The challenges associated with sediment loads are expected to worsen as weather extremes and the hydrologic cycle intensify under global climate change. NYCDEP has already documented an increase in high turbidity events linked to more frequent extremes and continues to invest in advanced sediment control in the Catskills region [NYCDEP, 2016]. Diagnostic assessments are necessary to contextualize past variability of suspended sediments, understand the watershed and climate mechanisms that control these variations, and inform models that can project suspended sediment concentrations under future projections of climate and land use change. Sediment-discharge rating curves are often coupled with long records of discharge data for this purpose, but recently these models have been found to exhibit nonstationary behavior and break down during and following major floods [Warrick et al., 2013; Yellen et al., 2014; Gray et al., 2015a,b], impairing their use in climate change adaptation assessments of sediment management strategies. The goal of this research was to develop improved models of suspended sediment loadings during and after extreme events and both demonstrate and promulgate their use in sustainable water management planning under

nonstationary climate in NYS. We focused on trends and variability in the flow-sediment relationship of the Esopus Creek that supplies drinking water to NYC and is a critical natural resource for communities in Ulster County.

Study #1

Modeling Experimental Design

In the first study, we used dynamic linear models (DLMs) to explore how the relationship between daily discharge and turbidity in the Esopus Creek has changed over the period between 1987-2015. DLMs are a class of state space model that represent a set of observations (i.e., suspended sediment concentration, load, or turbidity) as the sum of one or more latent (unobservable) state variables and observation noise, the latter often taken as the combination of measurement, sampling, and residual misspecification errors [Harrison and West, 1999]. The latent states are designed to capture the underlying (i.e., process-level) changes to the system that drive variations in the data beyond the observational noise. In the rating-curve application forwarded here, the underlying processes considered are changes in the relationship between turbidity and flow. This is modeled by letting the rating curve parameters be latent variables that vary in time and are inferred from the available observations. The DLM is defined by observation and state equations:

$$\log Ts_t = \beta_{0,t} + \beta_1 \log Q_t + \epsilon_t \qquad \epsilon_t \sim \mathcal{N}\left(0, \sigma^2_{\epsilon,t}\right)$$

$$\beta_{0,t} = \beta_{0,t-1} + w_t \qquad w_t \sim \mathcal{N}(0, \sigma^2_w)$$

Here, Ts_t is the observed turbidity load (turbidity×flow) at time t, Q_t is discharge, β_1 is the slope parameter, $\beta_{0,t}$ is a latent intercept, ε_t is the observation error, and w_t is the state evolution error. The DLM framework was applied in a case study examining changes in turbidity load in the Esopus Creek watershed, part of the New York City drinking water supply system. In this application, we only allowed the intercept ($\beta_{0,t}$) of the regression to change over time, and examine its temporal variability to better understand dynamics in sediment yield.

Results

Figure 2(a) shows the daily time series of the dynamic intercept from October 01, 1987 through September 30, 2015. We found that the dynamic intercept exhibits a complex array of variability across scales. For instance, the dynamic intercept exhibits a clear seasonality, as shown by the power spectrum for the 12-month period in Figure 2(b). However, the strength of this annual cycle varies over the period of record, suggesting that seasonal dynamics are not constant over long time scales. There is also significant and episodic oscillatory behavior in the 4-8 month band. Interestingly, these oscillations coincide somewhat with some of the largest flow events on record, depicted by vertical lines and tick marks in Figure 2. This indicates that large floods may initiate a longer-lived response in Ts yield beyond the peak in Ts associated with the large flow event. Overall, the large fluctuations in the intercept would suggest that, even after controlling for variability in discharge, there is a substantial amount of variability in Ts yield over the 29-year record.

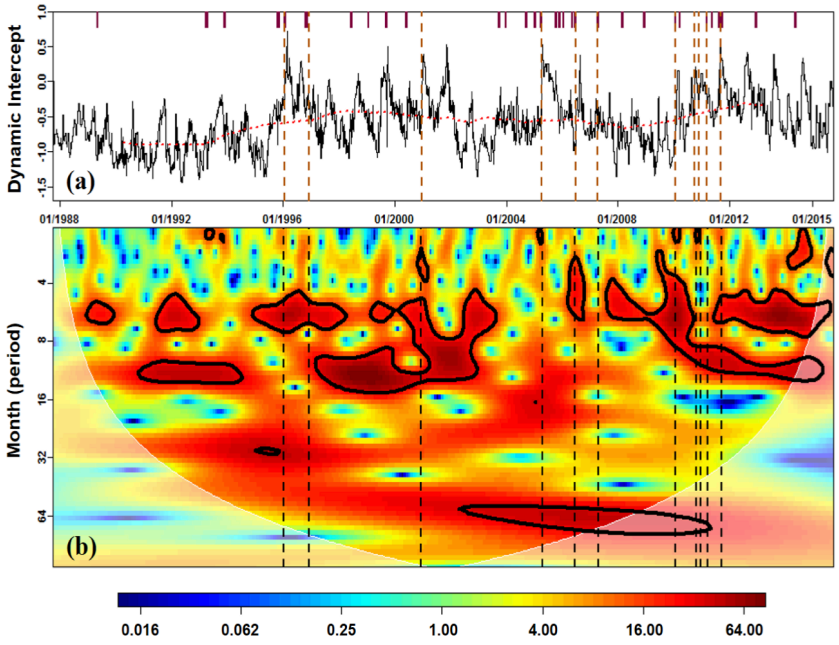

Figure 2. Intercept parameter of the DLM, including (a) daily time series plot along with its 5 year moving average (red dotted line) and (b) power spectrum for monthly averaged β_0 values, with bolded regions delimiting significance at the 90 % level. Vertical dotted lines mark the date of large floods (> 350 m^3/s). Small ticks at the top of (a) mark medium floods (> 204 m^3/s, i.e., the 99.5th percentile of daily flows).

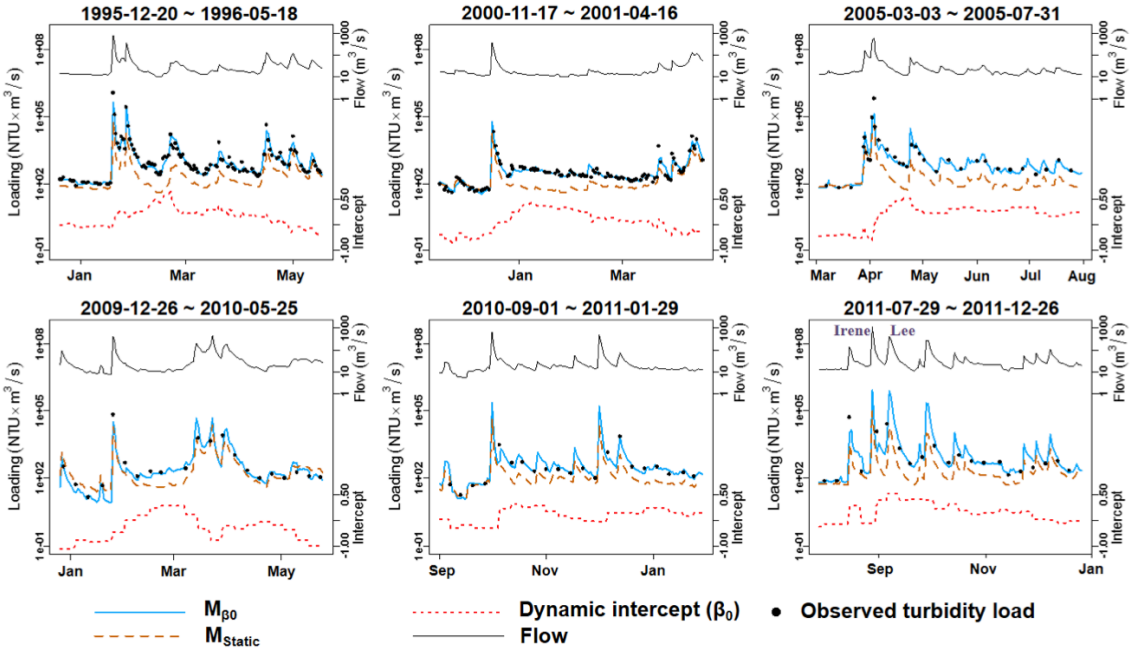

Figure 3. Observed turbidity loading with model predictions from $M_{\beta 0}$ and M_{Static} during six of the largest flood events on record. Here, hurricanes Irene and Lee are also denoted in the bottom-right pane. Time series of daily streamflow and β_0 are also shown.

Figure 3 shows observed Ts prior to, during, and after the six largest flood events recorded in the Esopus Creek at the Coldbrook gage for the sampled period of record, along with loading predictions under the DLM ($M_{\beta 0}$) and a static rating curve model (M_{Static}), the time series of discharge, and the time series of β_0. After each event, β_0 drifts higher and remains elevated for a prolonged period of time. Following certain floods (Jan. 1996, Apr. 2005, Aug. 2011), β_0 remained elevated above pre-flood values for over four months. Correspondingly, $M_{\beta 0}$ tends to capture Ts variability following these floods better than M_{Static}. These results suggest a degree of flood event-driven positive hysteresis in turbidity loads. This is thought to be linked to stream bank erosion and mass wasting that persist for prolonged periods after the flood [Yellen et al., 2014; Dethier et al., 2016]. These effects are simulated by the dynamic intercept. From the viewpoint of short- and medium-term load predictions, it is critical to capture such behavior, particularly if large floods occur in close succession. Otherwise, loadings may be severely under-predicted for the later storms.

Study #2

Modeling Experimental Design

The DLM results above indicate important variations in the rating curve between discharge and turbidity load in the Esopus Creek. However, because the DLM is effectively a time series filter, it cannot be used to model this behavior outside of the historical record of sediment data, as is commonly required in climate change impact studies. Therefore, we developed six rating curves of increasing complexity (M_1 through M_6) to provide a basis for evaluating whether the behavior captured by the DLM can be parameterized into a rating curve that would be appropriate for modeling flood-induced hysteresis under future climate change scenarios (Table 1). All models utilize two covariates including log-transformed discharge and seasonality, and are used to predict suspended sediment concentration (SSC) instead of turbidity. The first model, M_1, presents a baseline rating curve with just these two variables. M_2 employs a first order autoregressive (AR) term, which can flexibly capture short-term memory in the system but is not necessarily associated with hysteresis dynamics during high flow events. M_3 represents short-term hysteresis using the first difference of log(Q). The fourth model, M_4, utilizes a latent, time-varying intercept term β_0^* to represent long-term hysteresis following major flood events. The behavior of this latent intercept is designed to capture changes to SSC driven by mass wasting of steep cut banks that persists for prolonged periods after a flood. This model abstracts the flood-induced hysteretic behavior inferred from the DLM above. M_5 considers both short and long-term hysteresis simultaneously, combing the first order autoregressive term and the time-varying intercept of models M_2 and M_4, respectively. Similarly, M_6 adds the first time derivative of discharge used in M_3 to the structure of M_4.

TABLE 1 Model formulations of six rating curve models

Model	Model equation	Time-varying intercept
M_1	$\log rSSC_t = \beta_0 + \beta_1 logQ_{wt} + \beta_2 \sin(2\pi i_t) + \beta_3 \cos(2\pi i_t) + \varepsilon_t$	No
M_2	$\log rSSC_t = \beta_0 + \beta_1 logQ_w + \beta_2 \sin(2\pi i_t) + \beta_3 \cos(2\pi i_t) + \beta_4 \log\widehat{Q_{st-1}} + \varepsilon_t$	No
M_3	$\log rSSC_t = \beta_0 + \beta_1 logQ_w + \beta_2 \sin(2\pi i_t) + \beta_3 \cos(2\pi i_t) + \beta_5 \frac{dlogQ_{wt}}{dt} + \varepsilon_t$	No
M_4	$\log rSSC_t = \beta_0 + \beta^*_{0,t-1} + \beta_1 logQ_{wt} + \beta_2 \sin(2\pi i_t) + \beta_3 \cos(2\pi i_t) + \varepsilon_t$	Yes
M_5	$\log rSSC_t = \beta_0 + \beta^*_{0,t-1} + \beta_1 logQ_{wt} + \beta_2 \sin(2\pi i_t) + \beta_3 \cos(2\pi i_t) + \beta_4 \log\widehat{Q_{st-1}} + \varepsilon_t$	Yes
M_6	$\log rSSC_t = \beta_0 + \beta^*_{0,t-1} + \beta_1 logQ_{wt} + \beta_2 \sin(2\pi i_t) + \beta_3 \cos(2\pi i_t) + \beta_5 \frac{dlogQ_{wt}}{dt} + \varepsilon_t$	Yes

$$\beta^*_{0,t} = \varphi_1 \beta^*_{0,t-1} + \varphi_{2,t}(\log Q_{wt} - \log Q_{threshold})$$

$$\varphi_{2,t} = \begin{cases} 0 & \forall Q_{wt} < Q_{threshold} \\ \gamma & \forall Q_{wt} \geq Q_{threshold} \end{cases}$$

A comparison between M_1, M_2, and M_3 enables us to test the benefit of modeling different aspects of short-term memory in the system, including structured memory targeted specifically for event-based hysteresis. By comparing M_4 to the previous models, we can determine the utility of our formulation for long-term hysteresis, while a comparison of M_4 with M_5 and M_6 will highlight the benefits that emerge when considering both short- and long-term hysteresis effects simultaneously.

Finally, a climate risk assessment is presented to explore how these different formulations influence the analysis of water quality risk under plausible scenarios of alternative climate and hydrology. We utilize a partial duration model of peak flow events to compare SSC simulations between rating curves under alternative hydrologic scenarios. We first identify historical flow events greater than the value of $Q_{Threshold}$ calibrated for M_6. Inter-event timing between these events is modeled using an exponential distribution, and the magnitude of exceedances over the threshold is modeled using a Generalized Pareto distribution. The frequency and magnitude of new sequences of peak flows are then simulated through random draws from these distributions, and SSC for a subset of rating curve models is estimated for each event. Importantly, we consider two versions of M_6 in this experiment: 1) the original version calibrated from historical data, and 2) an altered version that uses the fitted parameters from the original version but suppresses any time-varying behavior in the latent intercept ($\beta_0^* = 0$ for all time steps). This approach enables a direct assessment of how the latent intercept impacts SSC during consecutive flood events.

Results

Figure 4 shows 2D histograms between observed and estimated SSC for the entire record using the six nested models. M_1 clearly underestimates the most extreme SSC values, while M_2 and M_3 show some improvement but still underestimate the largest values. Accordingly, both M_2 and M_3 generally have lower AIC values than the M_1 values, with M_3 modestly outperforming M_2. This suggests that an accounting of memory effects, particularly short-term hysteresis, improves predictions overall and to an extent also helps in the reproduction of extremes.

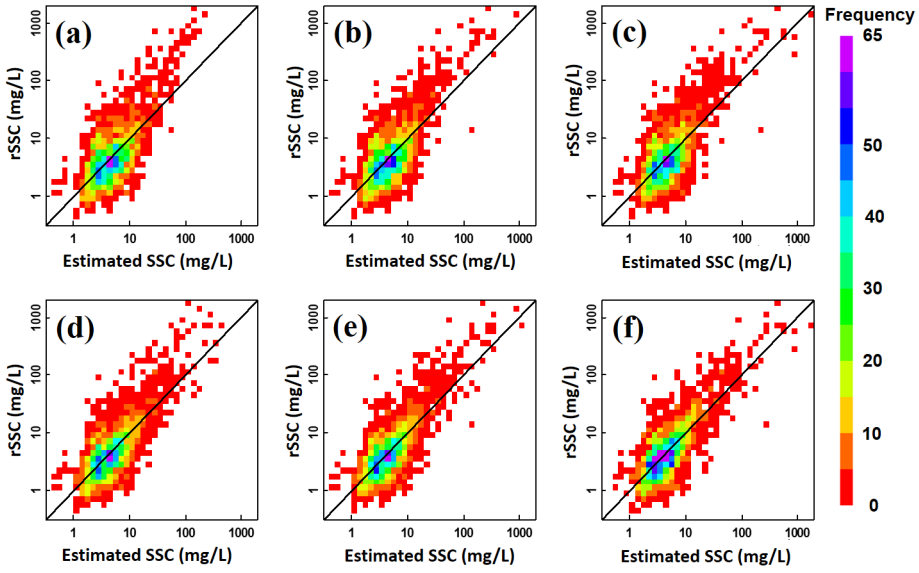

Figure 4. 2D histograms between observed SSC (rSSC) and modeled SSC estimated by (a) M_1 (b) M_2 (c) M_3 (d) M_4 (e) M_5 and (f) M_6.

Compared to M_1-M_3, M_4 generally performs better on the log-scale data, but this is not the case in the original scale. This suggests that M_4 is able to capture some post-flood behavior in the data better than the other models, but high SSC predictions are not as robust under the formulation. This can be seen in Figure 4d, which shows more scatter in high SSC predictions under M_4 compared to the previous models. Extreme SSC values are better represented when the long-term hysteresis in M_4 is coupled with additional terms to account for shorter-term hysteresis and additional system memory (M_5, M_6). We note that the fitted values of α_1 (all $\alpha_1 = 0.98$) in M_4-M_6 are consistently quite high, indicating substantial long-term memory following large floods. Both M_5 and M_6 improve performance over all other models when compared in logarithmic space. In the original scale, the results are more mixed, but overall M_6 tends to outperform the other models. M_6 also appears to show the least systematic bias for large SSC values (Figure 4). We therefore conclude that M_6 provides the most robust predictions of the six models tested.

We also examine the impact of the latent intercept and long-term hysteresis on extreme SSC estimates using flood simulations under a partial duration series approach. Figure 5 shows random samples of flood exceedances over $Q_{threshold}$ (fitted for M_6) for a future five-year period, given exponential and GPD distributions fitted to historical inter-event timing and magnitudes. Note that daily flow between each flood is not generated in this example. We consider four rating curve formulations including M_1, M_3, M_6 and M_6^*. Here, M_6^* uses the fitted parameters from M_6 but suppresses any time-varying behavior in the latent intercept. A comparison between M_6 and M_6^* allows for a direct assessment of how long-term hysteresis impacts extreme SSC estimates.

In Figure 5a, M_1 consistently produces the lowest SSC under all peak events. M_3 and M_6 produces higher estimates although the predictions are somewhat lower in M_3 than in M_6. M_6 also produces higher estimates than M_6^* after some events, like in 2020 and 2023, but not others. The difference emerges because of the dynamic intercept β_0^*, whose time-varying behavior is shown in Figure 5b. β_0^* remains elevated after the first flood in 2020 and 2023, increasing the estimate for M_6 during the second flood in each year. This highlights how the risk profile of extreme SSC fundamentally changes for a relatively brief (several month) window after major floods, which should be considered when considering how to manage water systems following these events.

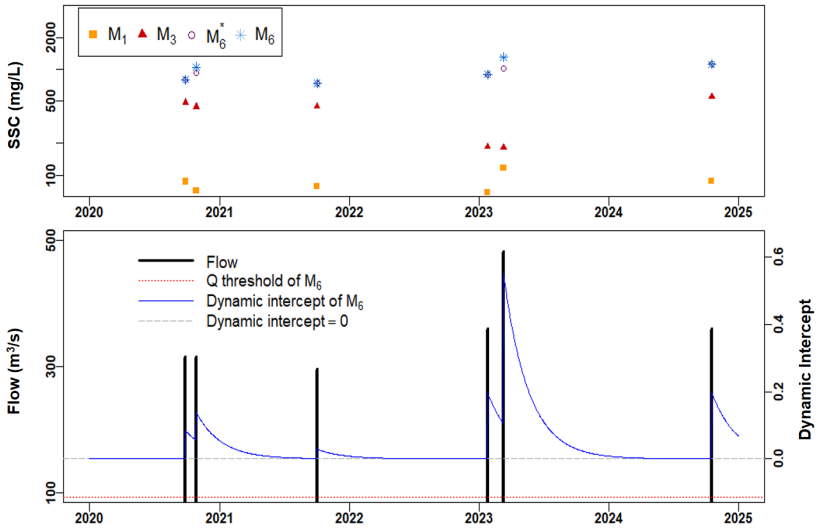

Figure 5 (top) Simulated SSC under M_1, M_3, M_6 and M_6^* for floods generated using the partial duration model. (bottom) Simulated floods (black) and corresponding changes in β_0^* (blue).

Conclusion

This work provided two primary contributions to the field of sustainable water resource management in NYS under climate change. First, it elucidated the capacity of multi-scale (daily to decadal) climate processes to shift discharge-sediment load rating curves used to characterize and predict suspended sediment in fluvial systems. Because basin sediment yield information is generally considered a static datum, documenting the mechanisms by which yields vary at different time scales comprises a major addition to our understanding of denudation and sediment delivery to reservoir systems, as well as other systems dependent on sediment inputs such as estuaries and coastal environments. Second, this work developed an innovative, transferrable modeling framework to simulate how sedimentation and other potential suspended constituent pollutants vary across time scales in response to different aspects of climate variability and change. Both research products were developed in conjunction with agency partners at NYCDEP in the Upper Esopus Creek Watershed in order enhance the application of these products and provide guidance for their design.

References

Dethier, E., F. J. Magilligan, C. E. Renshaw, and K. H. Nislow (2016), The role of chronic and episodic disturbances on channel–hillslope coupling: the persistence and legacy of extreme floods, Earth Surf. Process. Landf., 41(10), 1437–1447, doi:10.1002/esp.3958.

Gray, A.B., et al., (2015a), Effects of antecedent hydrologic conditions, time dependence, and climate cycles on the suspended sediment load of the Salinas River, California, J. Hydrol., 525, 632-649.

Gray, A.B., et al., (2015b), The effect of El Niño Southern Oscillation cycles on the decadal scale suspended sediment behavior of a coastal dry-summer subtropical catchment, Earth Surface Processes and Landforms, 40, 272-284.

Harrison, J., and M. West (1999), *Bayesian Forecasting & Dynamic Models*, Springer.

NYCDEP (2016), Watershed protection program summary and assessment, 2016 Filtration Avoidance Determination Assessment Report, 393 pp.

Warrick, J.A., et al., (2013), Trends in the suspended-sediment yields of coastal rivers of northern California, 1955-2010, J. Hydrol., 489, 108-123.

Yellen, B., et al., (2014), Source, conveyance and fate of suspended sediments following Hurricane Irene. New England , Geomorphology, 226, 124-134.

Otsego Lake Water Quality Constant Monitoring System

Basic Information

Title:	Otsego Lake Water Quality Constant Monitoring System
Project Number:	2017NY240B
Start Date:	3/1/2017
End Date:	2/28/2018
Funding Source:	104B
Congressional District:	NY-19
Research Category:	Water Quality
Focus Categories:	Water Quality, Surface Water, Education
Descriptors:	None
Principal Investigators:	Kiyoko Yokota, Paul Lord

Publications

There are no publications.

THIS PROJECT HAS RECEIVED A NO-COST-EXTENSION DUE TO DELAYS IN PROJECT FUNDING, AND DOES NOT CURRENTLY HAVE A FORMAL PROGRESS REPORT; However, an abstract for a planned presentation on current work is provided below

Abstract submitted to the North American Lake Management Society annual symposium in Nov 2018

Kiyoko Yokota, State University of New York College at Oneonta / Biological Field Station
Paul H. Lord, State University of New York College at Oneonta / Biological Field Station

Continuous Lake Monitoring Buoy – Lessons Learned from the First Year

Continuous lake monitoring buoys, or lake data buoys, once mainly developed and used by academic researchers, are gaining popularity within the greater lake management communities, including municipal utility operators and individual lake associations. These buoys log and transmit high-frequency data that reveal previously unnoticed spatial and temporal patterns in physical, chemical and biological processes in lakes and reservoirs. Established commercial vendors are capable of configuring a system that meets specific monitoring needs of a given site; however, the actual deployment method and maintenance needs are highly site specific and need to be carefully planned and executed by the local project managers. We present a case study from Otsego Lake, a glacial mesotrophic lake (maximum depth ≈ 51 m or 168 ft) in Central New York State, where we completed the first cycle of deployment, winterization and re-deployment of our NSF-funded data buoy in 2017-2018 as part of the Global Lake Ecological Observatory Network (GLEON). System configuration processes, initial and recurring cost, data management and analysis will also be covered. (169 words, 250 words max)

Preferred format: either oral or poster

Quantifying the ecosystem services of nitrogen removal and carbon sequestration in restored urban tidal wetlands

Basic Information

Title:	Quantifying the ecosystem services of nitrogen removal and carbon sequestration in restored urban tidal wetlands
Project Number:	2017NY241B
Start Date:	3/1/2017
End Date:	2/28/2018
Funding Source:	104B
Congressional District:	NY-12
Research Category:	Biological Sciences
Focus Categories:	Wetlands, Water Quality, Management and Planning
Descriptors:	None
Principal Investigators:	Chester Zarnoch

Publications

There are no publications.

Quantifying the ecosystem services of nitrogen removal and carbon sequestration in restored urban tidal wetlands

New York State Water Resources Institute

Final Technical Report

Sub-Award#78963-10874

Submitted by:

Chester B. Zarnoch, Ph.D.

Baruch College, City University of New York

30 April 2018

Title: *Quantifying the ecosystem services of nitrogen removal and carbon sequestration in restored urban tidal wetlands*

Summary:

Large scale wetland restoration efforts are common worldwide, and often motivated towards regaining lost ecosystem services such as nitrogen (N) removal and carbon (C) sequestration. Despite large monetary investment in wetland construction, research on the capacity for restored wetlands to retain C and remove N in eutrophic environments lags far behind. It is critical, however, to document these ecosystem services to help justify costs of restoration. In 2015-16 NYC Parks completed an assessment of 22 restored tidal wetlands in NYC that included measurements of habitat value and marsh structure but did not quantify N assimilation, N removal, or C sequestration. We measured C and N pools, and N fluxes including denitrification at four restored tidal wetland sites in the Harlem River.

We expected differences among sites due to varying ages (4 years to 15 years post-restoration) and associated wetland community development. The results, however, show that there were few differences in wetland structure and function across sites. Rates of denitrification were high at all sites and averaged 465 µmol $N\ m^{-2}\ h^{-1}$. These rates are higher than other reported values for natural and restored marshes suggesting that restored wetlands are hot spots for N removal in the Harlem River. The wetlands were also a sink for dissolved inorganic N (N retained rather than recycled), however, two of the four sites were sources of reactive P to the ecosystem likely due to reduced sediment. Overall, nitrogen removal and retention at these sites is very high and should be considered an important ecosystem service provided by these restored habitats.

We found high above and belowground biomass of the salt marsh plant, *Spartina alterniflora*, at all sites. The high belowground biomass and accumulation of sediment carbon led to significant C sequestration at each of the sites. The wetlands sequestered an average of 50 metric tons of C per acre which would have an economic value of $2,000 per acre. The C sequestered at Harlem River wetlands is similar to values reported in natural wetlands suggesting this is also an important ecosystem service provided by the restored habitats.

Future studies should consider seasonal differences in N cycling to better resolve estimates of annual N removal. Ongoing efforts aim to integrate the data into indices of marsh health with New York City Parks.

Study sites: The Harlem River is designated as Class "I" by the NYS Department of Conservation due to high inputs of nutrients and pathogens from wastewater effluent and combined sewer overflows (Fisher 2016). However, it is also a site within the Environmental Protection Agency's Urban Waters Federal Partnership which aims to connect urban communities to their local waterways by enhancing restoration efforts and improving the ecosystem services these sites provide. There have been four tidal wetland restoration projects in the Harlem River watershed including Swindler's Cove (SC; restored 2002), Little Hell Gate (LHG; restored 2006), Bronx Kill (BK; restored 2007), and Inwood Park/Muscota Marsh (MM; 2013). Measurements were taken at all sites in summer/early fall 2017.

A map of the project area in New York City. The proposed research will be conducted at four restored tidal wetland sites in the Harlem River (highlighted in red). The Harlem River is an 8-mile tidal strait connecting the Hudson River and East River. The river separates Manhattan and the Bronx.

Swindler's Cove (SC) marsh in September 2017 (left) and January 2018 (right)

Little Hell Gate (LHG) marsh in July 2016.

Bronx Kill (BK) marsh in July 2017.

Muscota marsh (MM) at Inwood Park in July 2017.

Research question #1) *Are restored wetlands nitrogen (N) and carbon (C) sinks under eutrophic conditions?*

Nitrogen flux measurements: We collected four intact sediment cores from each study site (n =16) on 21 September 2017 and brought these back to the laboratory at Baruch College. Lab incubations were set up according to An et al. (2001) using site water collected from each marsh. The water passed continuously over the cores at a rate of 1.1.ml h^{-1}. Inflow and outflow samples were taken after 24 hours. We then spiked the inflow containers with +20µM $^{15}NO_3^-$ and collected a second round of inflow and outflow samples after another 24h period (Zarnoch et al. 2017). The isotopic nitrogen enrichment served two purposes. First, it allowed us to see how the system responded to an increase of NO_3^- simulating storm events. Second, it allowed us to calculate nitrogen fixation and estimate denitrification supported by water column NO_3^-. Dissolved N and phosphorous (P) were measured with a nutrient autoanalyzer and gases ($^{28}N_2$:Ar, O_2:Ar) with membrane inlet mass spectrometry (MIMS; Kana et al. 1994). From these data, we calculated N and P fluxes, sediment respiration, and denitrification. After flux measurements,

roots and rhizomes were separated from the core sediments, washed, and dried. Sediment subsamples will be used to measure bulk density, organic matter (LOI), and C:N ratio.

Example of a sediment core collected at Little Hell Gate marsh (left) and laboratory set-up of continuous-flow core incubations (above).

Results:

<u>Sediment Oxygen Demand</u>

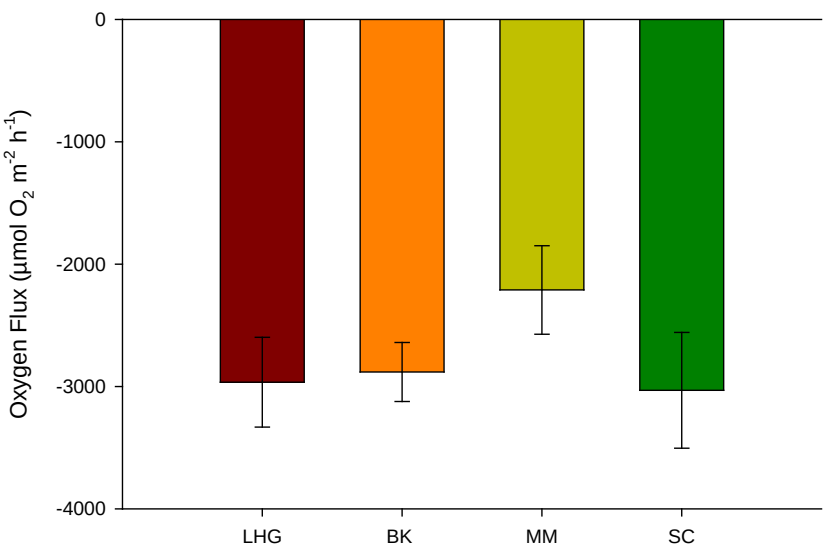

The sediment oxygen demand (O_2 flux) was similar among study sites.

Rates were similar to those reported for other tidal wetlands.

N_2 Flux

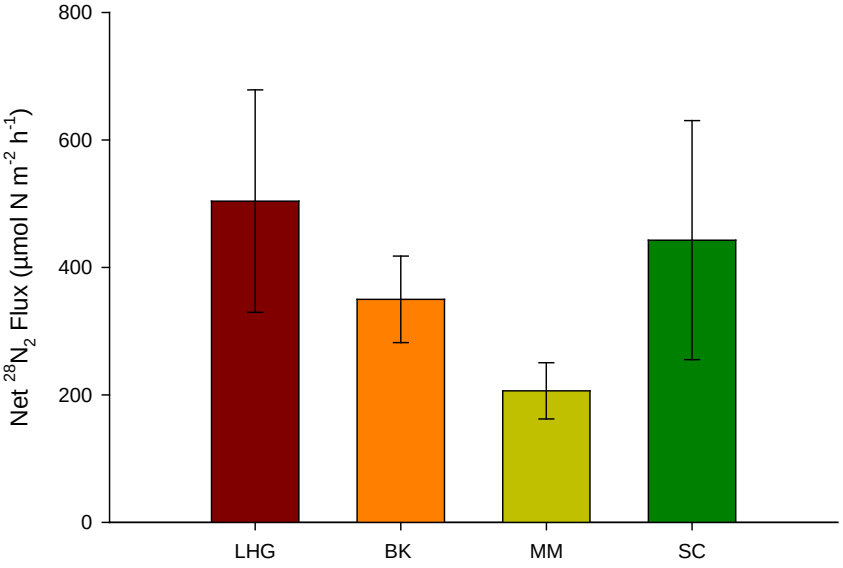

The net $^{28}N_2$ flux is a measure of net N_2 flux due to simultaneous processes of denitrification and N fixation. A positive flux indicates that denitrification was the dominant pathway.

The fluxes were statistically similar among sites.

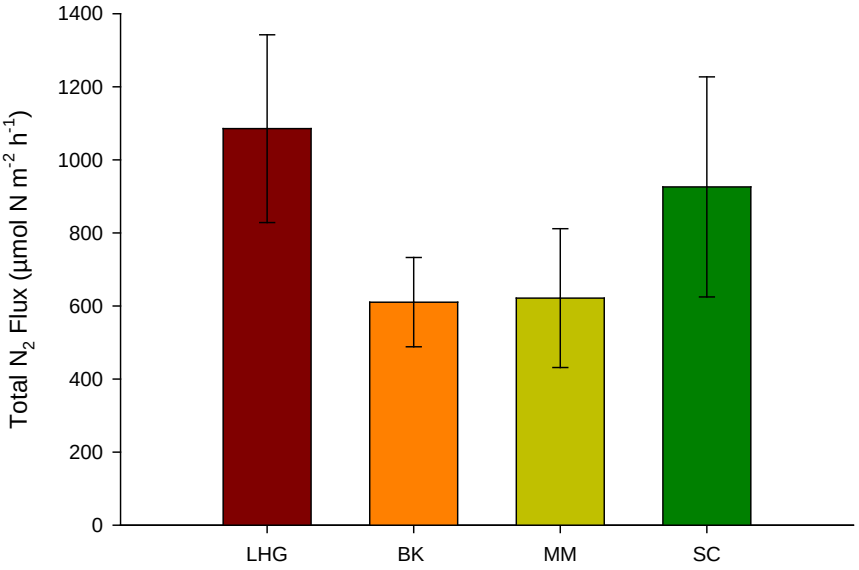

The total N_2 flux was measured from the $^{15}NO_3^-$ enrichment trial. It is indicative of potential denitrification.

The fluxes are greater here as compared to the $^{28}N_2$ fluxes indicating that the denitrifying community was NO_3^- limited.

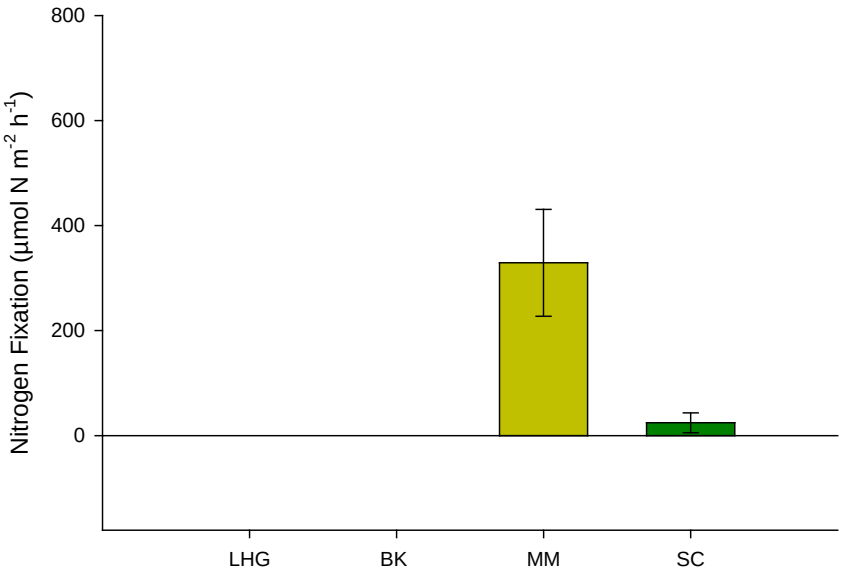

Nitrogen fixation was measurable at two sites. Rates were particularly high at Muscota marsh. Incubations were run in the dark so N fixation was likely due to sulfate and sulfide reducers or possibly methanotrophs.

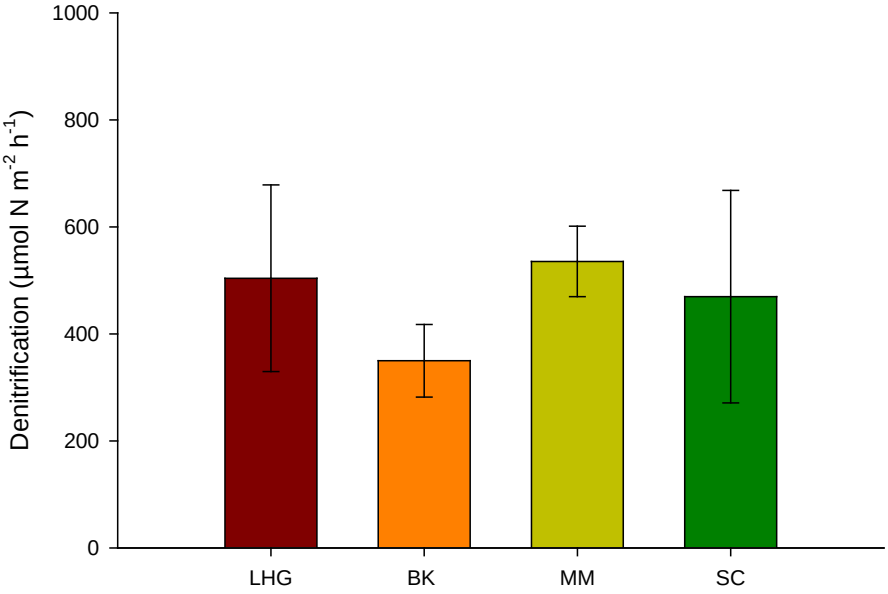

The denitrification rates were determined from the net $^{28}N_2$ fluxes while accounting for the observed N fixation.

Denitrification was very high and similar to or greater than rates reported for other natural tidal wetlands.

<u>Overall, the gas flux data show that the tidal wetlands in the Harlem River are important sites of nitrogen removal due to high denitrification rates.</u> Previous studies have indicated that it could take decades for restored marshes to have denitrification rates similar to natural marshes. The study sites have rates greater than natural marshes in as little as 4 years post-restoration.

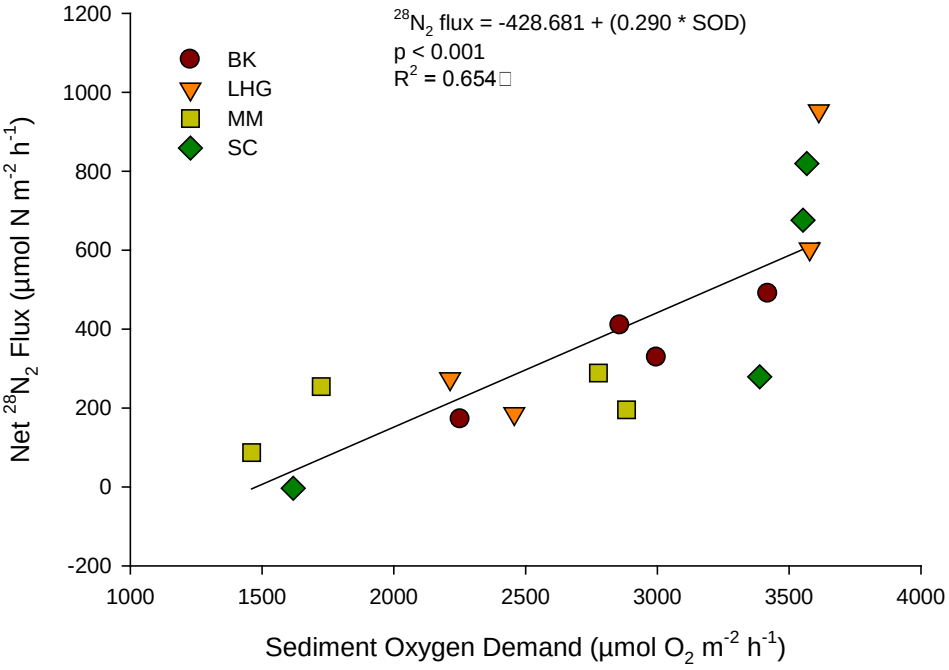

A positive relationship between SOD and N_2 flux is generally indicative of coupled nitrification-denitrification.

There is variability in this relationship across sites.

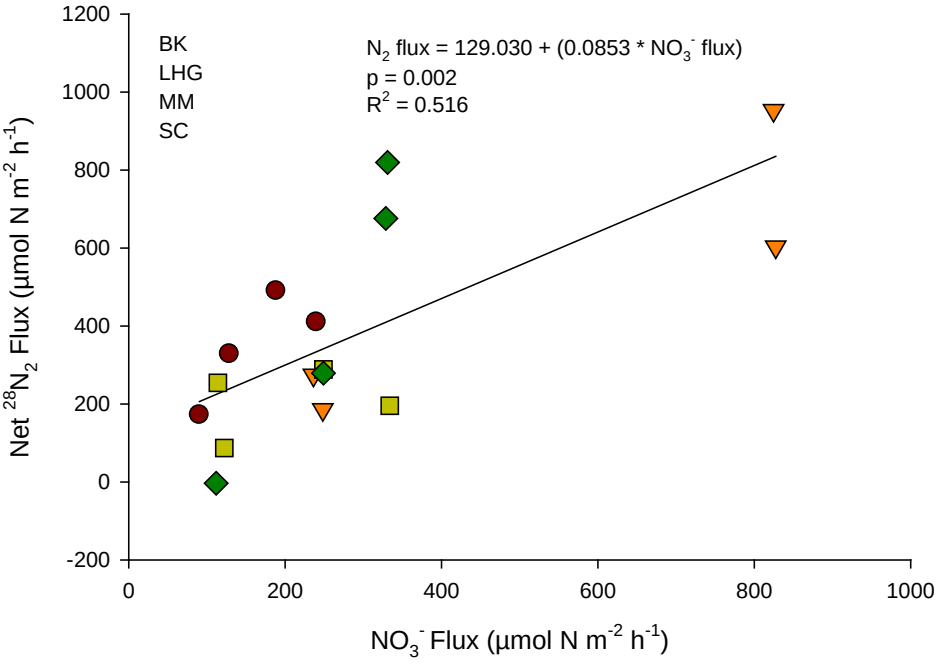

The positive relationship between NO_3^- and N_2 flux indicated that direct denitrification (use of water column NO_3^-) was also an important pathway of N removal.

Denitrification is supported by NO_3^- produced through sediment nitrification as well as by water column NO_3^-.

Nutrient Fluxes

A positive flux indicates a release of nutrients into the water column while a negative flux is indicative of sediment uptake of the nutrient.

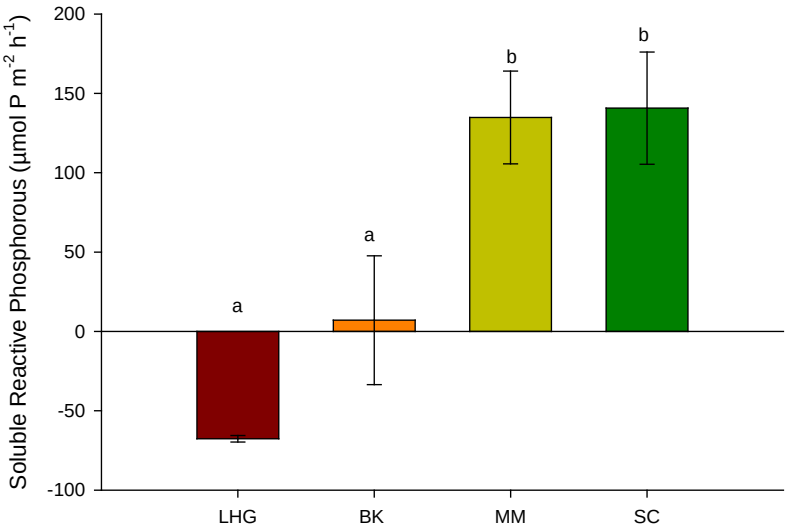

The phosphorous (P) flux was significantly different among sites. LHG had a net uptake of P while MM and SC had a very high release of P. The P flux at BK was negligible.

The high P flux at MM and SC was likely due to reduced sediments. Note this correlates with the N fixation data.

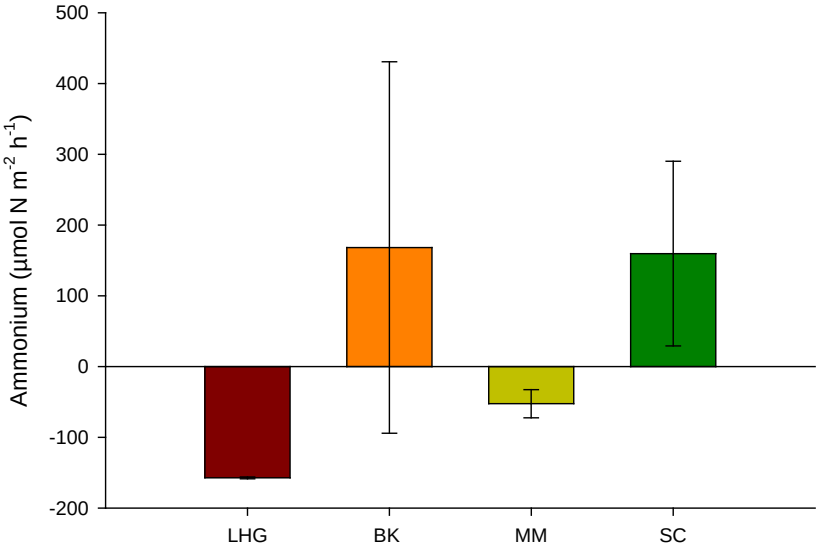

The ammonium fluxes were not statistically different among sites. LHG and MM showed an uptake of ammonium while SC had a release.

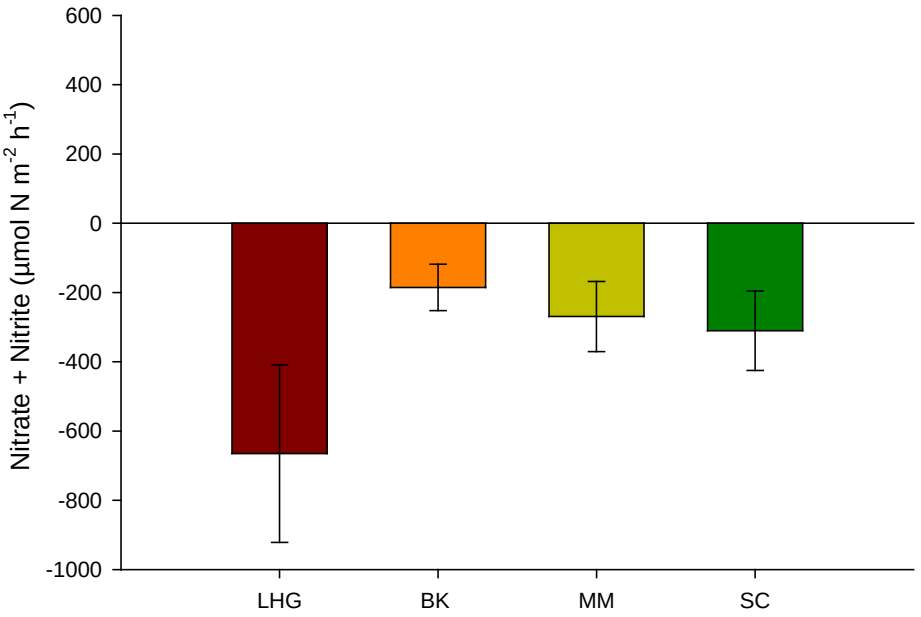

The NO_x^- fluxes (nitrate+nitrite) were negative indicating uptake of NO_x^-.

The fluxes are supported by high concentrations of water column NO_3^- in the Harlem River.

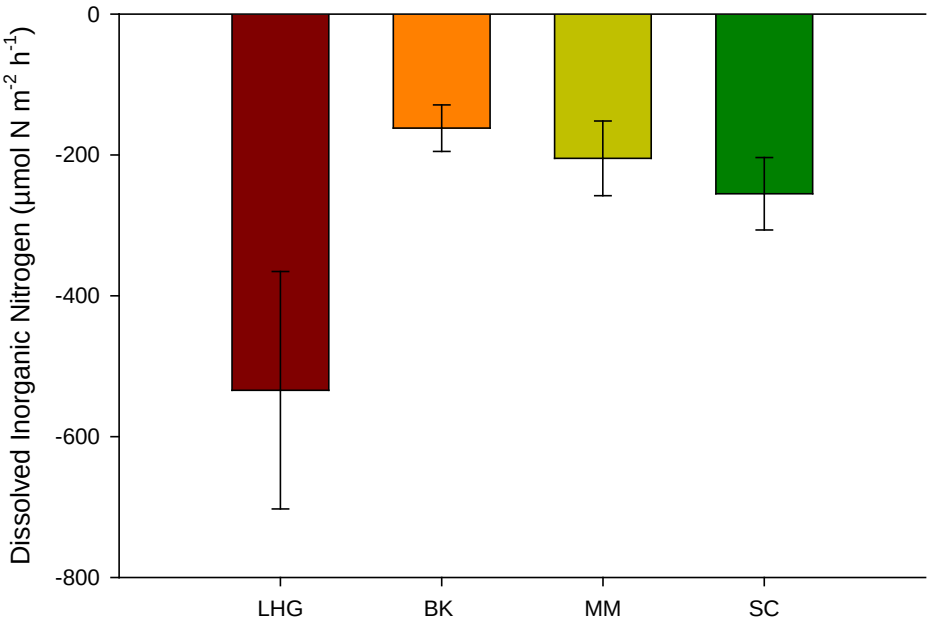

The total dissolved inorganic nitrogen (NH_4^+ + NO_3^-) fluxes were negative due to the dominant sediment NO_3^- uptake.

The nutrient flux data show that the study sites are sinks rather than sources of reactive N. However, we do note that MM and SC are sources of reactive P to the Harlem River. Sediment bound P may be released under reduced conditions.

Carbon (C) Fluxes

We measured carbon dioxide (CO_2) emissions from the wetland soils in early October 2017. We used a LI-COR LI-8100A automated soil CO_2 flux system following standard methods (Wigand et al. 2009, 2014). The system uses an infrared detector within a plastic dome placed in wetland sediments.

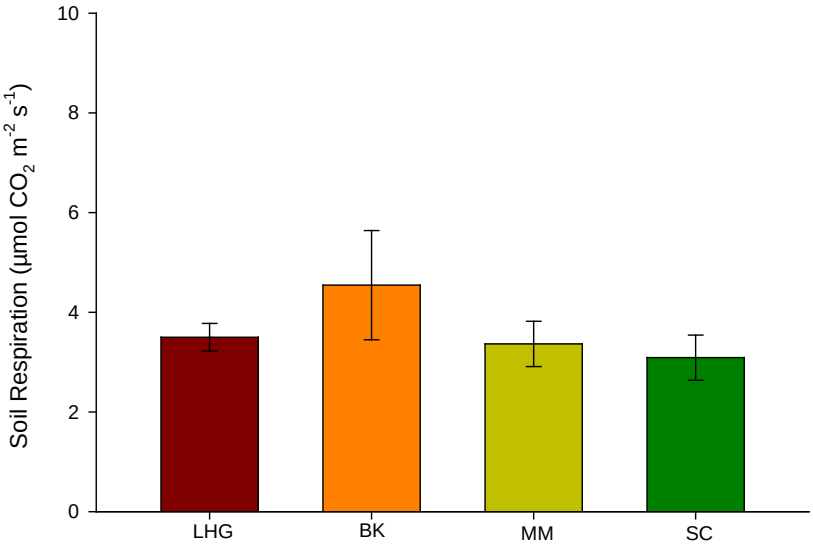

Soil CO_2 fluxes were similar among sites.

Rates observed in the Harlem River were similar to rates found in salt marshes from other eutrophic ecosystems. Rates are higher than pristine (nutrient poor) ecosystems.

Research question #2) *Are ecosystem services of N removal and C sequestration related to wetland structure or restoration design?*

Carbon pools and sediment characteristics. We measured the C pools at each study site in early October 2017. We haphazardly placed five 0.25 m^2 quadrats along the seaward edge of the tidal wetland. The salt marsh plant, *Spartina alterniflora*, was collected from each plot to determine stem height, density and biomass. We also collected a 2.76 cm diameter x 15 cm deep core from each quadrat to determine *Spartina* belowground biomass. Subsamples of root, above ground, and sediment were collected to determine 1) organic matter via loss on ignition (LOI), 2) C and N content using CHN Analyzer, as well as sediment bulk density. Generally, measurements of C sequestration in wetlands include cores down to a depth of 1 m, however, some of these restored sites are built upon rock fill and cores could not be taken deeper than 15cm.

Water chemistry and wetland flooding. Water column nutrients and chlorophyll *a* was measured biweekly at LHG and BK. We deployed HOBO data loggers within each site to quantify tidal inundation, salinity, and temperature.

Quantifying ecosystem services. We used our denitrification measurements to estimate the ecosystem service of N loss via denitrification and measurement of C pools for C sequestration at the wetland restoration sites in the Harlem River.

Wetland Vegetation Data

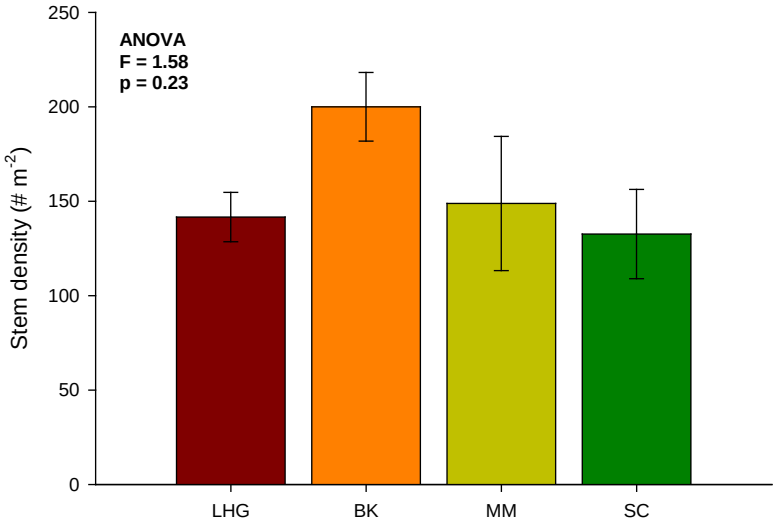

Stem density was similar among sites but are lower than densities reported for other restored and natural marshes.

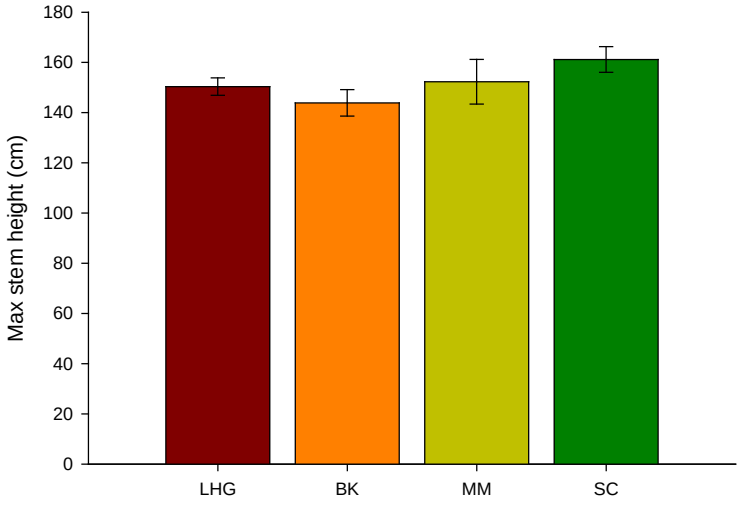

Spartina stem heights were similar among sites. Heights were greater than those found in restored marshes in Jamaica Bay, NY.

Therefore *Spartina* in the Harlem River grows taller than other ecosystems but this results in a lower density.

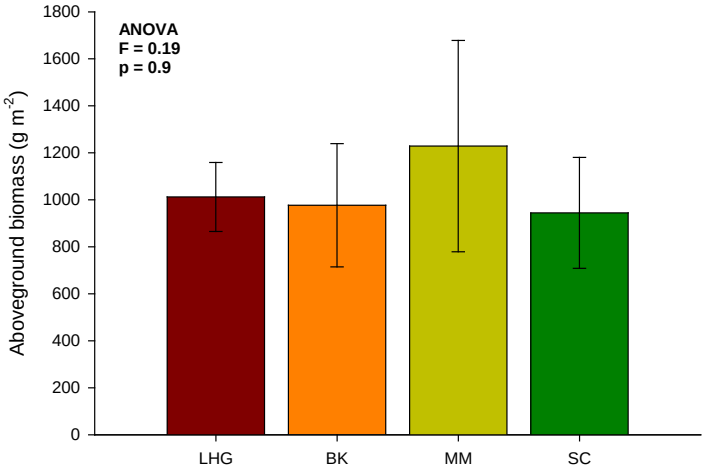

Total aboveground biomass was similar across study sites.

Biomasss was similar to natural marshes.

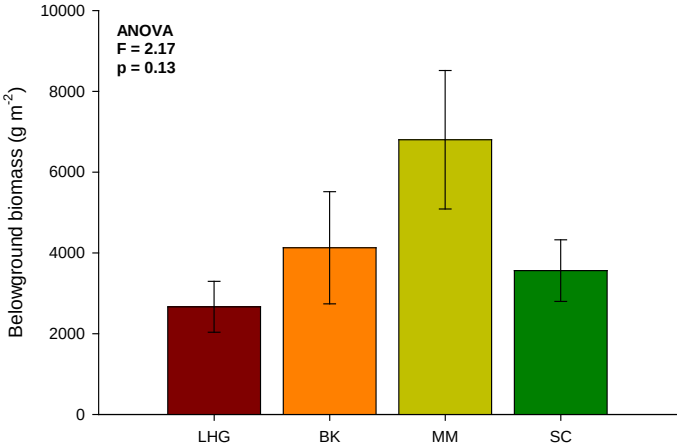

There was variation in belowground biomass found at each site, however, the differences were not statistically significant.

Belowground biomass at these sites were greater than wetlands of a similar age at Jamaica Bay.

Carbon Stocks

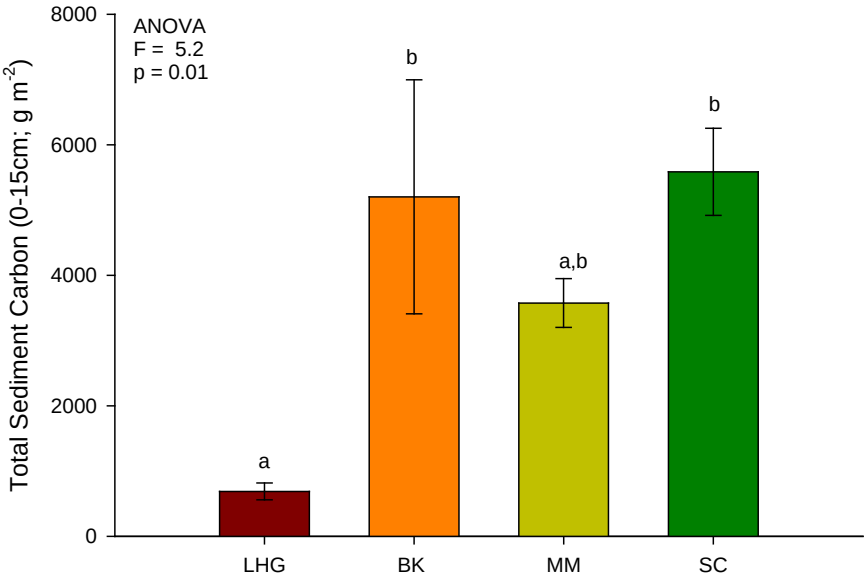

There were site differences in sediment C content with LHG having the lowest sediment C. The other three sites had sediment C similar to each other.

This was likely due to differences in sediment used in the construction of the sites as well as rates of C deposition.

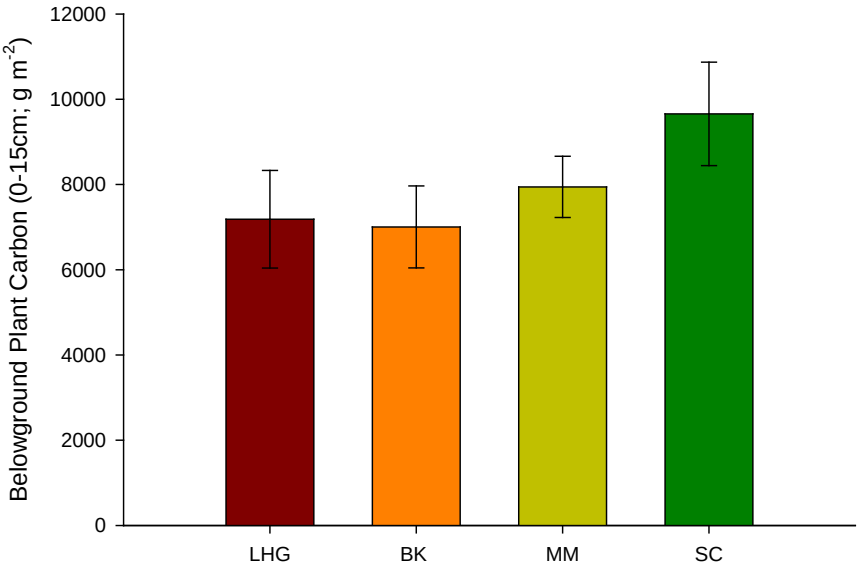

Belowground *Spartina* C was similar among sites as would be expected given similarities in biomass.

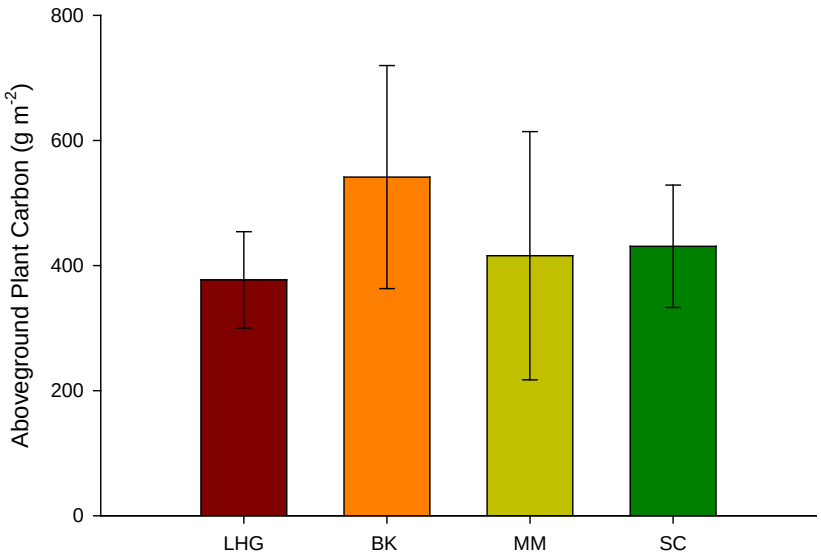

Spartina aboveground C was also similar among sites due to similarities in biomass and tissue %C.

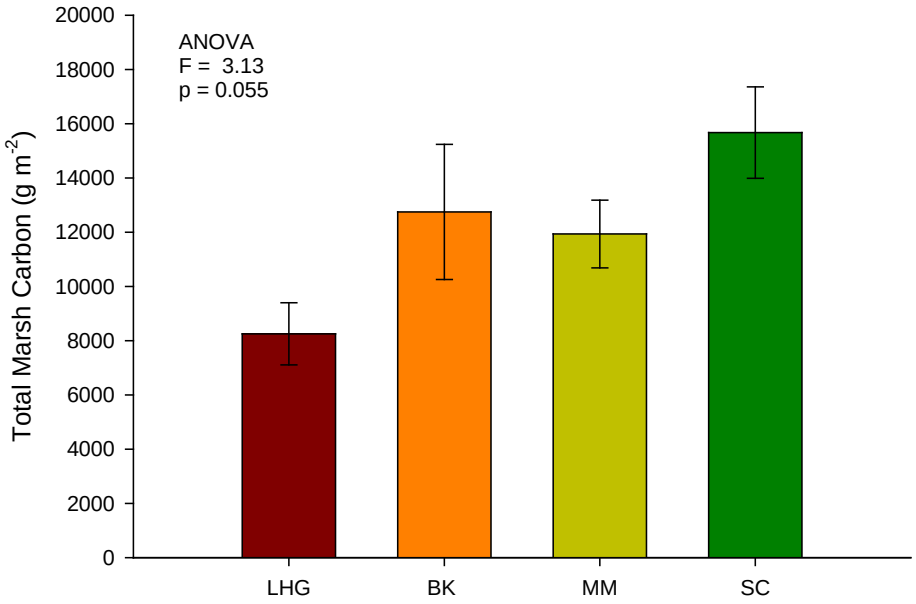

The total C sequestered in the tidal wetlands showed a marginal difference among sites with SC having the greatest and LHG having the lowest likely due to differences in sediment C.

The total carbon stocks found in the Harlem River sites are similar to stocks reported for other natural and restored tidal wetlands despite the samples only reaching a depth of 15cm. These data suggest that the Harlem River wetlands are important sites for C sequestration (i.e. blue carbon).

The measurement of carbon content in sediment is more time consuming and costly than determining organic content using the loss on ignition approach. To facilitate future estimates of sediment blue carbon in NYC restoration projects we determined the relationship between sediment organic content and sediment carbon.

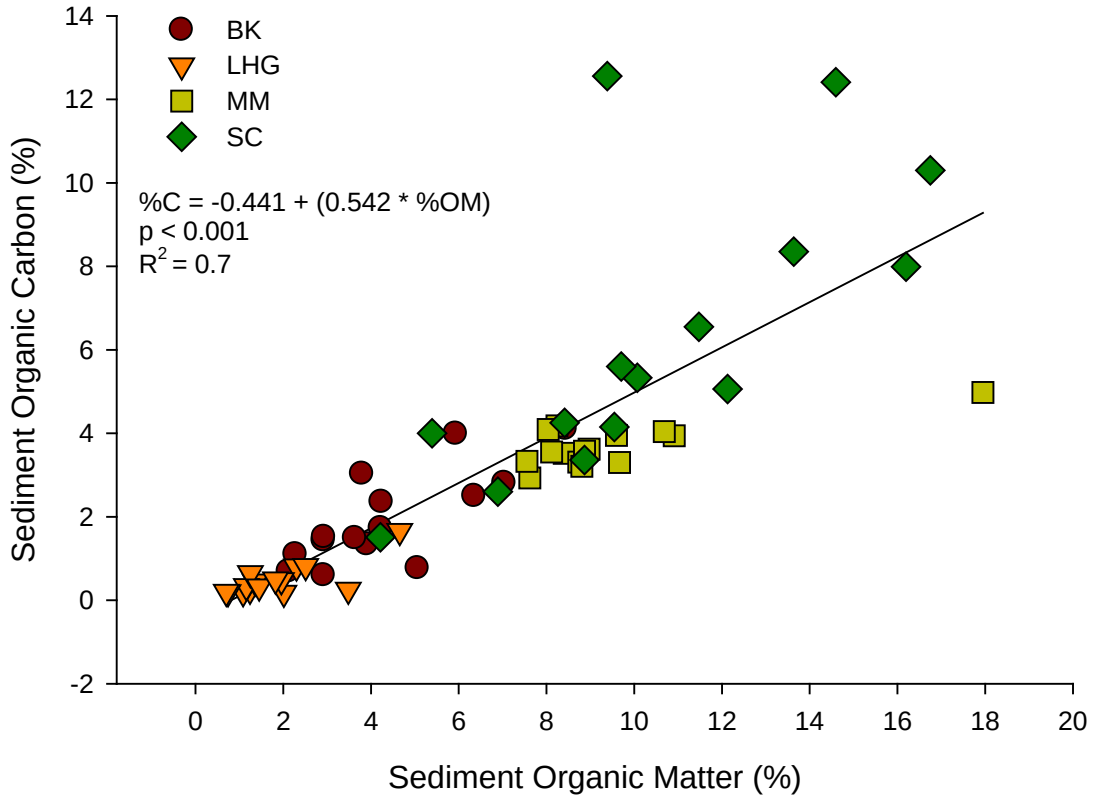

Nitrogen removal is related to sediment characteristics.

Rates of denitrification were similar across sites. We had hypothesized that rates would be influenced by differences in *Spartina* characteristics at each site but surprising these characteristics were also similar across sites despite different wetland ages. Sediment characteristics were different across sites. For example, LHG had much lower sediment carbon than BK and SC. We hypothesized that denitrification may be related to C since denitrifiers use C as an electron donor in the reduction of NO_3^-. However, we found no significant relationship with denitrification and sediment organic matter or sediment carbon. Lastly, we considered physical characteristics of the sediment and found a significant positive relationship (with one outlier removed) between sediment bulk density and net N_2 flux. This suggests that water flow through the sediment may be the important driver of denitrification rates. Low bulk density is associated with high organic matter and high porosity which results in less flow through the soils. The flow of water is critical for delivering water column NO_3^- or for moving O_2 through the soils for supporting nitrification.

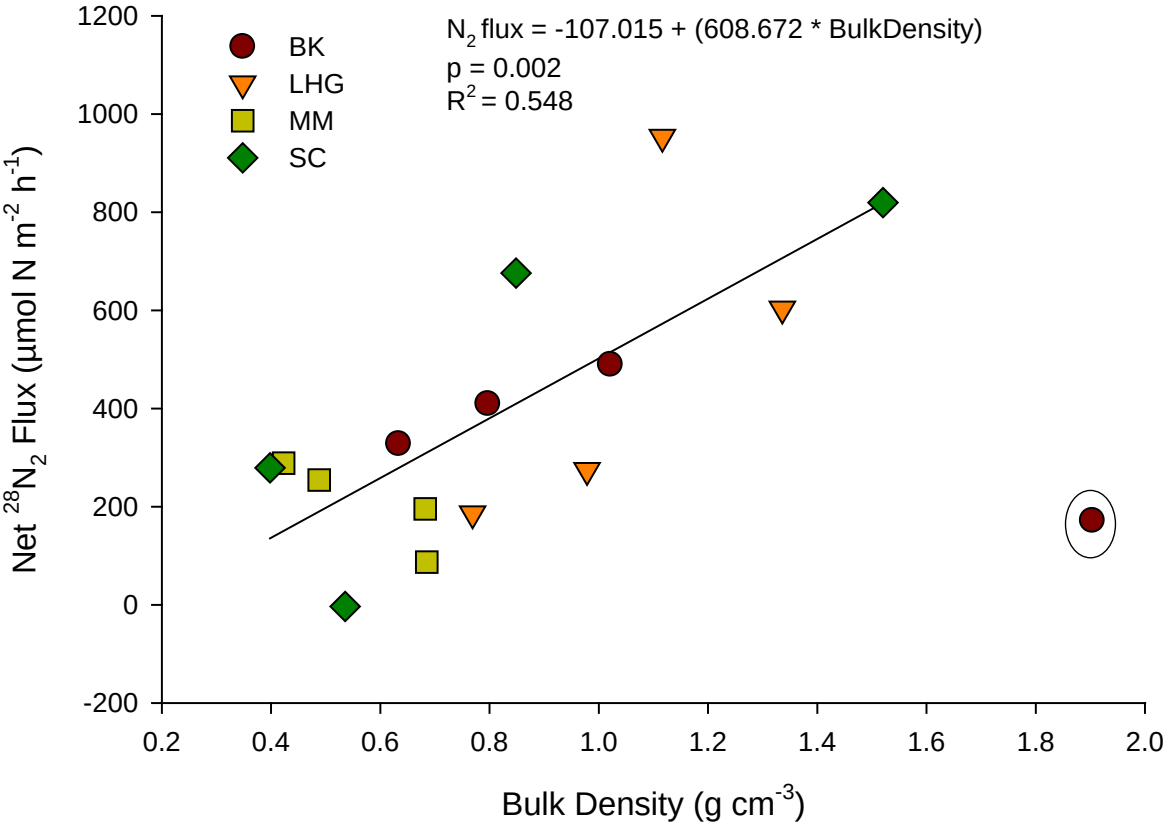

Tidal Inundation

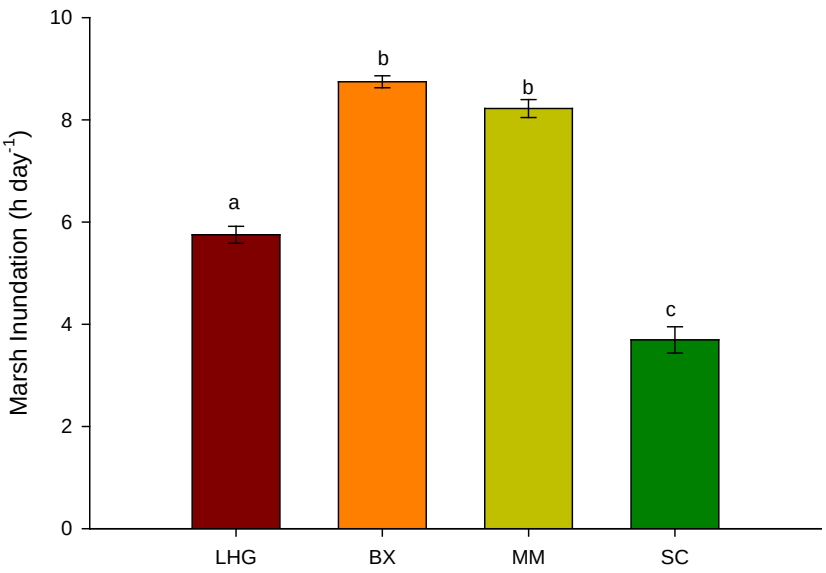

We used water level logger data to determine the average hours the wetlands were inundated by tides for each day. This is used as a proxy for elevation. Lower elevation wetlands get inundated more than higher elevation wetlands.

BK and MM were inundated the greatest amount of time per day. SC had the lowest inundation per day, however, several weeks of data were excluded from this analysis when ponding occurred in the wetland due to an accumulation of sediment at a creek mouth. Site managers need to ditch the wetland to promote drainage (see picture).

Ecosystem Service Calculations

Nitrogen Removal: We used our measurements of denitrification, tidal inundation, and wetland area to extrapolate wetland nitrogen removal to annual rates and estimate its economic value. We assume that our denitrification rate is constant year-round, however, rates are likely to vary across seasons and should be measured for more accurate estimates. Here we only consider DN when the marsh is inundated. We found that the wetlands can remove 60-400 lbs of N per year depending wetland area. The four study sites remove an average of 140 lbs of N per acre each year. The value of this N removal ranges from $90 to $2,200 per year when valuing N as in CT N trading programs (Zarnoch et al. 2017). The value of N removal would increase substantially when estimates of N removal for stormwater treatment ($500-$11,000) and wastewater upgrades ($120,000-$1,000,000) are used (Rose et al. 2015). Similarly, we could extend our measurements from when flooded only to 24h. Previous research has shown that wetland denitrification rates when submerged can be similar to when exposed to air. This would result in greater N removal rates and economic value.

Carbon Sequestration: We used our measurements of total carbon sequestered at each of the study sites to estimate blue carbon storage and economic value. The wetlands sequestered from 12 to 100 metric tons of carbon depending on wetland area. We used a value of $40 metric ton^{-1} of CO_2 (Macreadie et al. 2013) to estimate the economic value of wetland C sequestration to be $500 to $4,000. On average, we found that Harlem River wetlands sequester $2,000 worth of carbon per acre. Each acre of wetland would offset the annual CO_2 emission of 11 cars.

Project Outreach:

The project was a result of collaborations among Baruch College, Randall Island Park Alliance, New York Restoration Project, and New York City Parks' Natural Area's Conservancy. The relationships among these groups has been strengthened throughout the project. Randall Island Park Alliance has featured our work in social media posts and has been collaborating on wetland education programs. Baruch College has provided data and technical expertise to help guide an effort by New York Restoration Project to expand the size of the Swindler's Cove (SC) wetland. Baruch College is currently working with scientists from NYC Parks to exchange wetland data, evaluate health, and review design features.

Student Training

The project supported the participation of two CUNY graduate students, four undergraduates and one high-school student. Several of these students come from underrepresented groups in the geosciences. CUNY PhD student Jennifer Zhu participated in field and laboratory work while also receiving training in the use of membrane inlet mass spectrometry (MIMS) at Loyola University Chicago. This project as well as other ongoing studies on denitrification have helped convince Baruch College to purchase a MIMS for the Zarnoch lab. The machine will be arriving this spring and will support Jennifer's dissertation work. The project also supported CUNY PhD student Nathan Morris who is using metagenomics approaches to describe microbial community composition in restored wetlands. He aims to relate community composition to functional traits such as N removal. He may also use the MIMS in his dissertation work.

Top: PI Zarnoch and CUNY Ph.D. student Jennifer Zhu working at the Bronx Kill wetland. Bottom: Jennifer Zhu collected site water for continuous flow core incubations. Photos by Chris Girgenti of Randall Island Park Alliance.

Project funds were used for part-time research assistant positions for two CUNY undergraduate students. Renee Montelbano and Elizabeth Colon (pictured below) assisted in the field and laboratory analyses in fall 2017. They gained experience in vegetation and sediment analyses, water chemistry methods, elemental analyses as well as data analyses. Elizabeth has taken another laboratory position in CUNY working on green infrastructure. Renee continues to work in my lab but was recently hired by NYC Parks to work as a seasonal field coordinator.

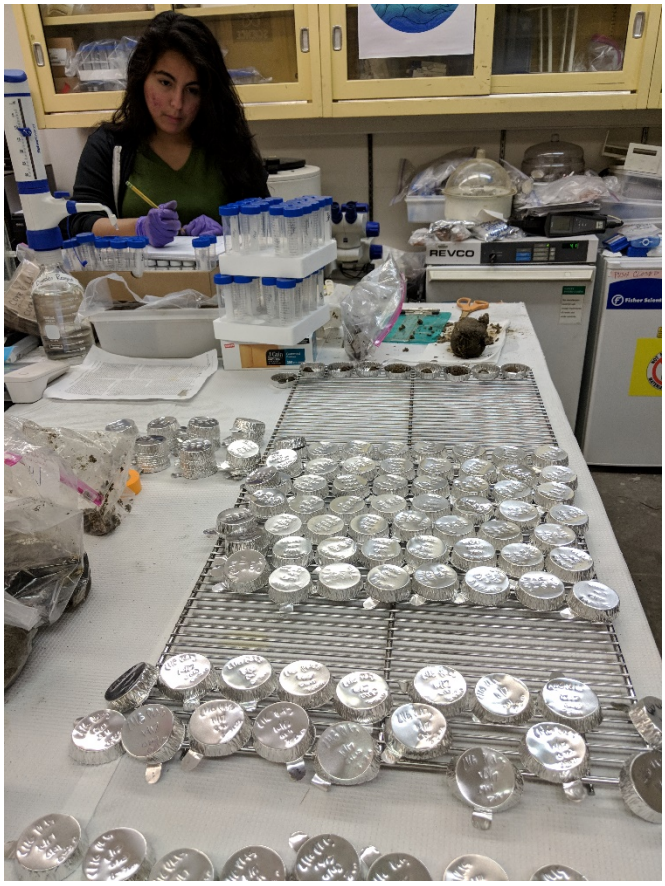

Esperanza Lima is an undergraduate at Baruch College working on the blue carbon data for an independent study (Credit based project). She is developing her paper and poster in collaboration with Renee. The project is titled, *"Blue carbon to make New York City more green- Urban salt marsh restoration as a means of carbon capture".* Lastly, Irina Vasilyuk has been working in the lab as a volunteer. Irina graduates in May 2018 and hopes to work for NYC Parks.

The project also supported the work of Tatiana Rampersaud (pictured below) who

is from the research program of Oceanside High School in Nassau County. Tatiana studied porewater nutrients, nitrification, and ammonification at the study sites during summer 2017. Her project was titled, "*Soil nutrients and transformations in New York City's constructed salt marshes*". Tatiana successfully presented her work at several science competitions in the NYC area.

Literature Cited:

An, S., W. S. Gardner, and T. Kana. 2001. Simultaneous measurement of denitrification and nitrogen fixation using isotope pairing with Membrane Inlet Mass Spectrometry analysis. Appl. and Environ. Microbiol. 67: 1171-1178.
Turner, R. E. 2009. Doubt and the values of an ignorance-based world view for restoration: coastal Louisiana wetlands. Estuaries and Coasts, 32:6 1054-1068

Fisher, S.C. 2016. Historical water-quality data from the Harlem River, New York. U.S. Geological Survey Scientific Investigations Report 2016–5044, 21 p., appendix, http://dx.doi.org/10.3133/sir20165044.

Kana T.M., C. Darkangelo, M.D. Hunt, J.B. Oldham, G.E. Bennett, and J.C. Cornwell. 1994. Membrane Inlet Mass Spectrometer for Rapid High-Precision Determination of N2, O2, and Ar in Environmental Water Samples. Analyt. Chem. 66: 4166-4170.

Macreadie PI, Hughes AR, Kimbro DL .2013. Loss of 'Blue Carbon' from Coastal Salt Marshes Following Habitat Disturbance. PLoS ONE 8(7): e69244. https://doi.org/10.1371/journal.pone.0069244

Rose, J. M., Bricker, S. B., & Ferreira, J. G. 2015. Comparative analysis of modeled nitrogen removal by shellfish farms. *Marine pollution bulletin*, *91*(1), 185-190.

Wigand, C., P. Brennan, M. Stolt, M. Holt, and S. Ryba. 2009. Soil respiration rates in coastal marshes subject to increasing watershed nitrogen loads in southern New England, USA. Wetlands 29:952–963.

Wigand, C., Roman, C. T., Davey, E., Stolt, M., Johnson, R., Hanson, A., ... & Rafferty, P. 2014. Below the disappearing marshes of an urban estuary: historic nitrogen trends and soil structure. Ecol. Appl., 24:4 633-649.

Zarnoch, C. B., Hoellein, T. J., Furman, B. T., & Peterson, B. J. 2017. Eelgrass meadows, Zostera marina (L.), facilitate the ecosystem service of nitrogen removal during simulated nutrient pulses in Shinnecock Bay, New York, USA. *Marine pollution bulletin*, *124*(1), 376-387.

PI Zarnoch examines a sediment core taken from Little Hell Gate marsh in New York City.

Information Transfer Program Introduction

The Director and staff of the NYS Water Resources Institute undertake public service, outreach, education and communication activities. Most are conducted through multidisciplinary projects funded outside the Water Resources Research Act (WRRA) context. In order to couple WRRA activities to other NYS WRI activities, a portion of WRRA resources are devoted to information transfer through a partnership program with the Hudson River Estuary Program, dissemination of information related to emerging issues, and student training.

Hudson River Estuary Program Partnership

Funded by the NYS Department of Environmental Conservation (DEC), the program is guided by 12 goals as part of its Action Plan formed in 1996. These goals address signature fisheries, river and shoreline habitats, plants and animals, streams and tributaries in the entire watershed, landscape and scenery, public access, education, waterfront revitalization, water quality, and partnerships and progress. WRI and DEC work together to protect this rich estuary ecosystem that is a source of municipal drinking water, spawning grounds for migratory fish, habitat for bald eagles, and an excellent recreation area for boaters, anglers and swimmers.

A summary of selected WRI information transfer activities is provided below For additional information on all activity, see wri.cals.cornell.edu

NYSWRI Publications
1. Water Resource Infrastructure in New York: Assessment, Management, & Planning – Year 5, Prepared October 24, 2017

Trade & Professional Publications
1. Lung, M., Meyer, A., Marjerison, R. and Rahm, B.G. “The Light at the End of the Culvert” Talk of the Towns, New York Association of Towns, 2017, 31, May/June, 18-22

Conference Presentations & Invited Talks
1. Truhlar AM (2017) Water institutes: Addressing water issues through research. Mid-Atlantic Water Resources Conference, National Conservation Training Center, Shepherdstown, WV. [oral presentation and town hall]
2. Truhlar AM (2017) Modeling culvert capacity in New York State. Congress of the Culverts, NYS DEC Region 3 Office, New Paltz, NY. (24 attendees)

Public Comments
1. Comments on the proposed rescinding of the 2015 Water of the United States rule, submitted by Chelsea Morris, James Knighton, Sheila Saia, Allison Truhlar, Brian Rahm, and M Todd Walter (NYS WRI) to the Federal Register, August 2017

Service
1. Participant in 2017 Town-Gown Resource Fair, Ithaca, NY
2. Speaker for 4H Career Explorations program, Water and Energy Literacy, June 28th, 2017, Ithaca, NY
3. Conference co-planner: 2017 Mid-Atlantic Regional Water Resources Conference, 2017, Sheperdstown, WV

USGS Summer Intern Program

None.

Student Support					
Category	**Section 104 Base Grant**	**Section 104 NCGP Award**	**NIWR-USGS Internship**	**Supplemental Awards**	**Total**
Undergraduate	7	0	0	0	7
Masters	1	0	0	0	1
Ph.D.	1	0	0	0	1
Post-Doc.	1	0	0	0	1
Total	10	0	0	0	10

Notable Awards and Achievements